Systems/Circuits

# When Norepinephrine Becomes a Driver of Breathing Irregularities: How Intermittent Hypoxia Fundamentally Alters the Modulatory Response of the Respiratory Network

**Sébastien Zanella,[1,2]* Atsushi Doi,[1,2]* Alfredo J. Garcia 3rd,[1,2] Frank Elsen,[1,2] Sarah Kirsch,[1] Aguan D. Wei,[1,2] and Jan-Marino Ramirez[1,2]**

[1]Center for Integrative Brain Research, Seattle Children's Research Institute, Seattle, Washington 98101, and [2]Department of Neurological Surgery, University of Washington, Seattle, Washington 98104

**Neuronal networks are endogenously modulated by aminergic and peptidergic substances. These modulatory processes are critical for maintaining normal activity and adapting networks to changes in metabolic, behavioral, and environmental conditions. However, disturbances in neuromodulation have also been associated with pathologies. Using whole animals (*in vivo*) and functional brainstem slices (*in vitro*) from mice, we demonstrate that exposure to acute intermittent hypoxia (AIH) leads to fundamental changes in the neuromodulatory response of the respiratory network located within the preBötzinger complex (preBötC), an area critical for breathing. Norepinephrine, which normally regularizes respiratory activity, renders respiratory activity irregular after AIH. Respiratory irregularities are caused both *in vitro* and *in vivo* by AIH, which increases synaptic inhibition within the preBötC when norepinephrine is endogenously or exogenously increased. These irregularities are prevented by blocking synaptic inhibition before AIH. However, regular breathing cannot be reestablished if synaptic inhibition is blocked after AIH. We conclude that subtle changes in synaptic transmission can have dramatic consequences at the network level as endogenously released neuromodulators that are normally adaptive become the drivers of irregularity. Moreover, irregularities in the preBötC result in irregularities in the motor output *in vivo* and in incomplete transmission of inspiratory activity to the hypoglossus motor nucleus. Our finding has basic science implications for understanding network functions in general, and it may be clinically relevant for understanding pathological disturbances associated with hypoxic episodes such as those associated with myocardial infarcts, obstructive sleep apneas, apneas of prematurity, Rett syndrome, and sudden infant death syndrome.**

*Key words:* **breathing; glycine; intermittent hypoxia; neuromodulation; preBötzinger complex; rhythmogenesis**

## Introduction

Neuromodulation is essential for the functioning of all neuronal networks (Doi and Ramirez, 2008; Harris-Warrick and Johnson, 2010; Garcia et al., 2011). Neuromodulatory substances are critical for organizing networks during development (Frederick and Stanwood, 2009; Kobayashi, 2010; Lee and Goto, 2011), maintaining network activity, and adapting neuronal networks to changes in metabolic, behavioral, and environmental conditions (Krugel et al., 2009; Harris-Warrick and Johnson, 2010). Moreover, neuromodulation plays a critical role in various forms of plasticity and metaplasticity (Sarnyai et al., 2000; Baker-Herman and Mitchell, 2002; Hart et al., 2011; Hu et al., 2011; Jitsuki et al., 2011). Therefore, it is not surprising that disturbances in neuromodulation have been associated with many neurological conditions, such as stroke, traumatic brain injury, multiple sclerosis, neuropsychiatric disorders, epilepsy, and Parkinson's disease (Frederick and Stanwood, 2009; Lusardi, 2009; Burnstock et al., 2011; Hasselmo and Sarter, 2011). Pathological changes in the abundance of neuromodulators are thought to be primarily responsible for a given clinical phenotype. For example, in Parkinson's disease, the loss of dopaminergic neurons seems to be responsible for most of the symptoms. Interventions to substitute for the lack of dopamine are the most effective treatments (Caiazzo et al., 2011; Katsnelson, 2011; Kriks et al., 2011). A disturbance in the abundance of neuromodulators may also contribute to breathing disturbances in Rett syndrome, in which norepinephrine (NE) content is decreased in areas of the brainstem (Viemari et al., 2005; Zanella et al., 2008).

In this study, we provide evidence that subtle changes in the configuration of a neuronal network may lead to fundamental changes in the responsiveness to neuromodulators, which have dramatic consequences on network functions. Specifically, our data suggest that network disturbances and consequently clinical phenotypes could be caused by the same endogenous neuro-

Received July 30, 2012; revised Nov. 7, 2013; accepted Nov. 9, 2013.

Author contributions: S.Z., A.D., and J.-M.R. designed research; S.Z., A.D., A.J.G., F.E., and S.K. performed research; A.D.W. contributed unpublished reagents/analytic tools; S.Z., A.D., A.J.G., F.E., and J.-M.R. analyzed data; S.Z., A.D., and J.-M.R. wrote the paper.

This work was supported by National Institutes of Health Grants R01 HL 099296 and P01 HL090554.

*S.Z. and A.D. contributed equally to this work.

Correspondence should be addressed to Dr. Jan-Marino Ramirez, Center for Integrative Brain Research, Seattle Children's Research Institute, 1900 9th Avenue, Seattle, WA 98101. E-mail: nino1@uw.edu.

DOI:10.1523/JNEUROSCI.3644-12.2014

 0270-6474/14/340036-15$15.00/0

modulators that, under normal conditions, stabilize network activity. Here we focused on the preBötzinger complex (preBötC), a well defined network within the ventrolateral medulla (Smith et al., 1991; Schwarzacher et al., 2011) that is critical for breathing. Lesioning of this network leads to the cessation of breathing (Ramirez et al., 1998b; Gray et al., 2001; Tan et al., 2008). Isolated in brainstem slice preparations, the preBötC continues to generate different types of respiratory activity resembling those of normal respiratory activity, gasping and sighing (Smith et al., 1991; Lieske et al., 2000; Peña et al., 2004). The preBötC is endogenously modulated by NE, and noradrenergic neurons are located within its close vicinity (Ellenberger et al., 1990; Viemari and Ramirez, 2006; Zanella et al., 2006). Here we specifically show that subtle changes in the configuration of the respiratory network fundamentally alter the modulatory response to NE. Indeed, NE, which is normally stabilizing respiratory network activity (Blanchi and Sieweke, 2005; Zanella et al., 2006), becomes a driver of irregularity. This fundamental change in the responsiveness is caused by exposing the respiratory network to brief repeated periods of decreased oxygen levels (hypoxia). We refer to this stimulus as acute intermittent hypoxia (AIH). Episodes of hypoxia occur in a large number of pathologies, such as myocardial infarcts, obstructive sleep apneas, chronic bronchitis, apneas of prematurity, Rett syndrome, and sudden infant death syndrome. Although the present study was performed in the respiratory network, we believe that the finding that a modulatory response can fundamentally change after intermittent hypoxia has general implications for other neuronal networks as well.

## Materials and Methods

All animal experiments were performed with the approval of the Institute of Animal Care and Use Committee of the Seattle Children's Research Institute. Mice were maintained with rodent diet and water available *ad libitum* in a vivarium with a 12 h light/dark cycle at 22°C.

### *Transverse brainstem slice preparation*

In all *in vitro* experiments, transverse 600-$\mu$m-thick brainstem slices containing the preBötC were obtained from CD-1 mice (males and females, 6–9 d old) as described previously (Ramirez et al., 1996). Briefly, mice were anesthetized with 4% isoflurane and quickly decapitated at the C3/C4 spinal level. The brainstem was dissected in ice-cold artificial CSF (aCSF), equilibrated with carbogen (95% $O_2$–5% $CO_2$, pH 7.4). The medulla was sliced using a microslicer (VT1000S; Leica). Slices were submerged in a recording chamber (6 ml) under circulating aCSF (30°C; flow rate, 18 ml/min; total circulating volume, 100 ml). ACSF contained the following (in mM): 118 NaCl, 3 KCl, 1.5 $CaCl_2$, 1 $MgCl_2 \cdot 6H_2O$, 25 $NaHCO_3$, 1 $NaH_2PO_4$, and 30 D-glucose, equilibrated with carbogen. Extracellular KCl was elevated from 3 to 8 mM over a span of 30 min to initiate and maintain rhythmic population activity. Extracellular recordings were obtained with glass suction electrodes positioned on the slice surface in the area ventral to the nucleus ambiguus (NA), near or on top of the preBötC. The preBötC mainly contains spontaneously active inspiratory neurons and also few expiratory neurons (Ramirez et al., 1997b; Winter et al., 2009). However, the motoneurons in the hypoglossal nucleus (XII) that innervate the genioglossius are driven in-phase with inspiration. Thus, preBötC population bursts serve as markers of fictive inspiration and are in-phase with the population activity of XII neurons (Smith et al., 1991; Ramirez et al., 1997a). In some experiments, we recorded from both preBötC of the same slice or from one preBötC and the ipsilateral XII nucleus (Ramirez et al., 1997a, 1998a; Telgkamp and Ramirez, 1999).

### *Anesthetized freely breathing mouse preparation*

As described previously (Doi and Ramirez, 2010), CD-1 mice (P10–P23) were anesthetized with urethane (1.5 g/kg). Mice were placed in a supine position, and the head was fixed with a stereotaxic apparatus. The neck of the mice was opened from the ventral side, the trachea was cut, and a plastic Y-shaped tubing for supplying $O_2$ was inserted into the proximal end of the trachea (cannulation). The bone covering the ventral brainstem was partially removed with small scissors and forceps. In this preparation, the reverse Y-shaped basilar artery and the branches of the hypoglossal nerve could be observed. The dura and arachnoid membranes were removed to expose the ventral medulla. The surface of the ventral medulla was continuously perfused with 95% $O_2$–5% $CO_2$ equilibrated aCSF solution at 30 ± 0.5°C. Under control condition, 100% $O_2$ was supplied through cannulation without artificial ventilation.

### *Drugs and AIH*

*In vitro.* In all experiments, fictive inspiration was recorded for 15 min to obtain a control baseline with aCSF bubbled with carbogen (95% $O_2$–5% $CO_2$). Subsequently, slices were exposed to AIH, i.e., five bouts of 3 min exposure to aCSF bubbled with a mixture of 95% $N_2$–5% $CO_2$ separated by 3 min reoxygenation with carbogen (Fig. 1). If not stated otherwise, drugs were applied during the 5 min period immediately preceding the first bout of hypoxia. Drugs were then continuously applied throughout the experiment.

An amperometric system consisting of custom-constructed platinum wire electrodes (Garcia et al., 2010) and a polarographic amplifier (model 1900; A-M Systems) was used to measure the $PO_2$ in the preparation bath. Flush-tip electrodes were made by cutting (30–50 $\mu$m diameter) Teflon-insulated platinum wire (A-M Systems). The electrode was polarized to a potential of −700 mV with respect to an Ag/AgCl reference electrode placed in the bath. The electrode was calibrated at the beginning and the end of the day. Calibrations were performed in the slice bath using aCSF equilibrated with 0% $O_2$ (supplemented with the $O_2$ scavenger $NaSO_3$ to produce anoxia) and at three to five additional calibration points between 10% and 95% $O_2$. A second-degree polynomial function was used to define the calibration curve to convert amperometric measurements to $PO_2$ (Torr $O_2$). $PO_2$ was corrected for vapor pressure. On average, the bath $PO_2$ was 670 ± 20 Torr under control condition (95% $O_2$) and 35 ± 16 Torr at the end of the hypoxic bout (0% $O_2$). The core $PO_2$ values were estimated to be ~60 Torr under control condition and 5–10 Torr during the hypoxic bout as we showed previously (Hill et al., 2011).

*In vivo.* In all experiments, anesthetized mice were fixed in the stereotaxic apparatus during and after the acute surgery, which was performed from the ventral side of the medulla (Doi and Ramirez, 2010). After completion of the surgery, inspiratory activity was recorded from the intercostal muscles for 15 min to obtain a control baseline. Under control conditions, 100% $O_2$ was supplied through the cannula of the trachea. Mice were freely breathing and required no artificial ventilation. After 15 min of baseline recording, mice were exposed to AIH consisting of five bouts of isocapnic hypoxia that was generated by switching the supply of pure $O_2$ to a mixture of 95% $N_2$–5% $CO_2$ for 3 min. Each isocapnic hypoxic bout was separated by a 5 min reoxygenation period with 100% $O_2$ (see Figs. 6, 7). Arterial $O_2$ saturation ($SaO_2$) was monitored using the non-invasive MouseOx system (STAR Life Sciences) with the mouse thigh sensor. Signals were stored on a personal computer and analyzed offline. Figure 6*D* depicts a representative blood $SaO_2$ profile during an intermittent hypoxia protocol. On average (35 measurements), the arterial $SaO_2$ reached during an isocapnic hypoxic bout was 36 ± 4%, whereas it was close to 100% under normal condition.

Microsyringes (Hamilton microsyringe 80330) with a 33 gauge needle, containing either aCSF or drugs, were positioned with micromanipulators (KITE; World Precision Instruments). The needle was inserted into the right preBötC area from the ventral side. The drugs were applied 5 min before the first bout of hypoxia, and they were injected at a rate of 0.3 $\mu$l/min. We did not attempt to perform bilateral needle injections to limit the damages caused to the preBötC, which could have compromised respiratory rhythm-generating mechanisms.

These types of injection are performed routinely in our laboratory (Doi and Ramirez, 2010). In a subset of experiments ($n = 7$), we quantified the spreading of the drug by injecting Lucifer yellow fluorescent dye (1% LY, 0.4 $\mu$l; Invitrogen) into the preBötC using exactly the same approach as was performed in all our *in vivo* experiments. For these experiments, we took advantage of Cre/loxP mouse lines bred to condi-

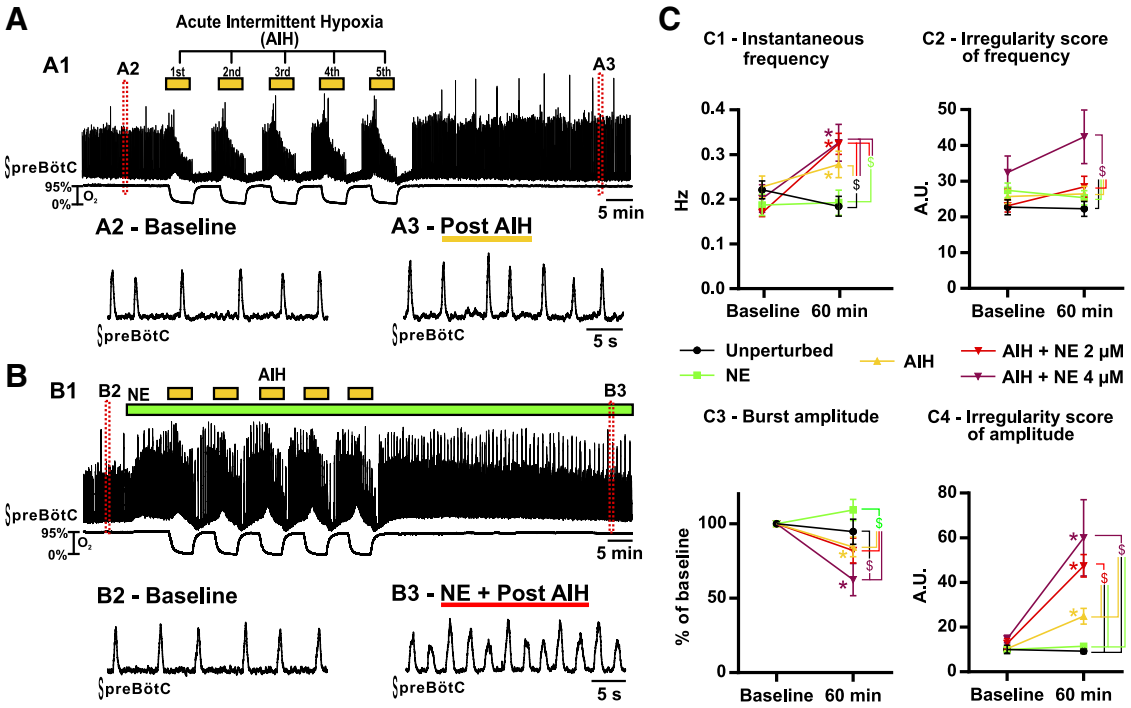


**Figure 1.** Fictive breathing activity recorded from brainstem slices *in vitro*. ***A***, Consequences of five bouts of 3 min hypoxia separated by 3 min of reoxygenation, i.e., AIH. ***A1*** shows the integrated activity recorded from the preBötC (top trace) and the $O_2$ level in the bath (bottom trace). Enlarged timescale of the fictive breathing activity before (***A2***) and after (***A3***) AIH. ***B***, Same as ***A*** but in the presence of NE. ***B1*** shows the integrated activity recorded from the preBötC (top trace) and the $O_2$ level in the bath (bottom trace). Enlarged timescale of the fictive breathing activity before (***B2***) and after (***B3***) AIH. ***C***, Parameters of the fictive breathing activity observed before AIH and/or drug injection (baseline) and 30 min after the last bout of hypoxia (or 60 min after baseline). The inspiratory burst instantaneous frequency (***C1***) and amplitude (***C3***) as well as the IS of frequency (***C2***) and amplitude (***C4***) were measured (number of slices in each condition: $n = 9$ unperturbed; $n = 8$ NE; $n = 15$ AIH; $n = 19$ AIH + NE at 2 $\mu$M; $n = 6$ AIH + NE at 4 $\mu$M). Note the significant increase of burst frequency and IS of amplitude in slices exposed to AIH and NE. Also note the significant increase of IS of frequency in slices exposed to AIH and NE at 4 $\mu$M (two-way ANOVA followed by Holm–Sidak *post hoc* test; * represents significant difference compared with baseline in one group; $ represents significant difference between groups at the same time; different levels of statistical differences are not represented).

tionally express Channelrhodopsin (H134R) fused to tdTomato from the Rosa26 locus [B6.Cg–*Gt(ROSA)26Sor*$^{tm27.1(CAG-COP4*H134R/tdTomato)Hze}$/J; Ai27], in all cholinergic neurons, by the expression of Cre recombinase under the control of the choline acetyltransferase promoter (B6;129S6–*Chat*$^{tm2(cre)Lowl}$/J; ChAT–cre; Madisen et al., 2012). Thus, we took advantage of the construct to easily label the NA. This nucleus is a well known landmark to locate the preBötC (Schwarzacher et al., 2011), which is located ventral of the NA. One hour after LY injection into the preBötC area, mice were killed with an overdose of anesthesia and perfused transcardially with PBS (0.1 M, pH 7.4), followed by paraformaldehyde (4% in PBS, pH 7.4) to fix the brainstem. Then, the brainstem was removed and sectioned (200 $\mu$m) using a vibratome. Each slice was visualized with a fluorescent microscope (Olympus SZX16), and LY spreading was measured using the NIH ImageJ software. Figure 6*A–C* represents the measurements obtained on a total of seven mice. Although the preBötC area shows the brightest staining, there is some spreading into surrounding regions.

Throughout this study, only one animal or one brainstem slice was used per experiment. All drugs were supplied from Sigma-Aldrich or Tocris Bioscience.

### *Intracellular recordings*

We used the visual-patch technique (Zeiss Examiner microscope with IR-Dodt optics) to obtain intracellular voltage-clamp recordings from inspiratory neurons that were active in-phase with the population burst recorded extracellularly from the preBötC (see Fig. 3*A*). The discharge pattern of each neuron was first identified in the cell-attached mode, and, in all cases, the discharge pattern remained similar after obtaining the whole-cell configuration. Experiments were then performed in the whole-cell patch-clamp mode. Neurons were first held at a holding potential ($V_H$) of −60 mV to identify their pattern of activity (Fig. 3*A1*). Then the $V_H$ was raised to −50 mV (Fig. 3*A2*) to allow for better recognition of spontaneous IPSCs (sIPSCs; Bouvier et al., 2008). Data were recorded continuously and every 5 min stored in separate files.

Recordings were made with unpolished patch electrodes, manufactured from borosilicate glass pipettes with filament (Warner Instruments G150F-4). The recording electrodes had resistances of 3–5 MΩ when filled with the pipette solution containing the following (in mM): 140 K-gluconate, 1 $CaCl_2$, 2 $MgSO_4$, 10 EGTA, 4 $Na_2ATP$, 0.3 Na-GTP, and 10 HEPES, pH 7.2. Neurons located directly at the slice surface were not examined because they were more likely to be severely damaged during the preparation than were neurons located deeper within the slice. Recordings with obvious space-clamp problems were discarded (Armstrong and Gilly, 1992). Poor space clamping was indicated by rebound spikes (rapid, fast inactivating inward currents that were induced by steps from depolarizing test potentials to the former $V_H$). Whole-cell patch-clamp recordings were obtained with a patch-clamp amplifier (Multiclamp 700B) at a sample frequency of 10 kHz and a low-pass filter setting of 2 kHz. Data were digitized with a Digidata 1400 (Molecular Devices) and analyzed offline using Mini Analysis software (6.0.7; Synaptosoft). For each 5 min data file, we generated an average for inhibitory (sIPSC) and excitatory (sEPSC) events. To generate an average event, first all events in the file were identified by the computer, and their accuracy was verified by the user. Then the computer randomly picked 75 events, which were superimposed and lined up at 50% rise time. The user then checked for correct alignment of the rising phase and an undisturbed falling phase of each event. Events that did not meet those criteria were discarded. The number of events used for the average was always trimmed down to 50 single events. The average events were fitted with a one-exponential function, and the results for amplitude and decay time (Tau) were transferred into a data table for additional analysis.

*Signal processing, data acquisition, and data analyses*

The population activity of both the preBötC and the XII was obtained from a signal containing multiunit action potential activity amplified 5000-fold and filtered between 100 Hz and 5 kHz using an extracellular amplifier (model 1700; A-M Systems). The signal was then rectified and integrated by using an electronic integrator with a time constant of 50 ms and subsequently digitized with a Digidata 1400 (Molecular Devices).

A Teflon-covered Ag bipolar electrode was used for electromyographic (EMG) recordings of the intercostal muscles. The skin over the abdominal and intercostal area on the right side was partially removed, and the bipolar electrode was placed on the surface of the intercostal muscle. Signals were alternating current amplified, bandpass filtered (8 Hz to 3 kHz), and digitized with a Digidata 1400 (Molecular Devices).

The signals were stored on a personal computer using pClamp 10 (Molecular Devices) software. The data were analyzed offline using Clampfit 10.

We measured the frequency, amplitude, and regularity of the inspiratory activity in both preparations. To describe the regularity of the activity on a burst-by-burst basis, we used the irregularity score (IS) as described previously (Barthe and Clarac, 1997; Telgkamp et al., 2002; Viemari et al., 2005; Ben-Mabrouk and Tryba, 2010). The formula for the IS of frequency is as follows: $IS_{Fr-N} = 100 \times ABS\,(P_N - P_{N-1})/P_{N-1}$, whereas $IS_{Fr-N}$ is the IS frequency score of the $N$th cycle, $P_N$ is its period, $P_{N-1}$ is the period of the preceding cycle, and ABS is the absolute value. In this study, we also apply this formula to assess the irregularity of burst amplitude $IS_{amp}$ by replacing in the previous formula the period by the amplitude of the integrated and rectified inspiratory burst (with unchanged time constants throughout the study). Noteworthy, the IS for both amplitude and period has no unit and is thus independent of the unit used to measure it; these are two advantages of using these variables. A low IS represents a regular rhythm, whereas a higher value represents a less regular rhythm in either frequency or amplitude. Sigh frequency was increased by NE application and could therefore increase the irregularity of both frequency and amplitude. Hence, sighs were discarded during the measurement of these irregularities to only obtain a measure for eupnea. However, sighs were included in the measurement of instantaneous frequency.

Two data bins of 5 min were taken from individual experiments: (1) the first data bin before experimental manipulation (i.e., 5 min after the beginning of the recording); and (2) the second after experimental manipulation (i.e., 30 min after the last bout of hypoxia in the case of AIH, or to match the timing of the experimental group exactly 60 min after the control bin).

*Statistical analyses*

Numerical data are presented as the mean ± SEM. The figures represent the raw values for respiratory frequency and irregularity under baseline and after the test. However, as it is usually done in the literature, signal amplitudes are normalized to baseline because these values are based on arbitrary units. These values depend, for example, on signal-to-noise ratio, the recording quality in each experiment, and the amplification. $N$ values represent the number of individual slices or mice from which the quantification was conducted. Differences between two means before and after a condition were determined by the paired Student's $t$ test. Differences between more than two means were determined using both the values under baseline and after the test using two-way ANOVA (treatment × time) and corrected for multiple comparisons by Holm–Sidak *post hoc* test ($t$ values are given in parentheses). All statistics were performed using GraphPad Prism 6. All differences were considered significant at $p < 0.05$.

## Results

### AIH fundamentally alters the response of the respiratory network to NE *in vitro*

Using spontaneously rhythmic slice preparations, we tested the long-term response of the preBötC to AIH ($n = 15$ slices), i.e., five 3-min-long exposures to 0% $O_2$ separated by 3 min intervals. At 30 min after hypoxic exposure, there was a significant increase in the instantaneous frequency (Fig. 1*A*,*C1*; $F_{(1,52)} = 28.33$; $p < 0.001$), as well as the amplitude irregularity ($IS_{amp}$) of fictive inspiratory bursts (Fig. 1*A*,*C4*; $F_{(1,52)} = 43.21$; $p < 0.001$). However, when compared with unperturbed slices ($n = 9$) at the same time, only the increase in frequency was statistically significant (Fig. 1*C1*; $t_{(104)} = 2.930$; $p < 0.05$).

It was shown previously that NE at a high dose (20 μM) acutely stabilizes the respiratory activity *in vitro* (Viemari et al., 2005; Viemari and Ramirez, 2006). Here we applied a smaller dose (2–4 μM) to rhythmically active slices ($n = 8$) and maintained the NE exposure for 70 min. These lower concentrations allowed us to apply the drug on a longer period of time while limiting the desensitization of the NE receptors. Besides, the same range of dose could be used both *in vitro* and *in vivo*. Although NE was initially excitatory and stabilizing, this effect was transient, and none of the parameters measured after 60 min were significantly different from unperturbed slices at the same time (Fig. 1*C*). We then tested the combined effect of NE (2 μM) and AIH ($n = 19$; Fig. 1*B*). At 30 min after hypoxic exposure in the presence of NE (2 μM), the instantaneous frequency of the inspiratory bursts increased significantly when compared with baseline (Fig. 1*B*,*C1*; $t_{(52)} = 8.689$; $p < 0.001$). This frequency increase was also highly significant when compared with unperturbed slices ($t_{(104)} = 4.074$; $p < 0.001$) and slices exposed to NE alone ($t_{(104)} = 3.686$; $p < 0.01$; Fig. 1*C1*). Most pronounced, the $IS_{amp}$ was significantly higher in slices exposed to AIH and NE when compared with baseline (Fig. 1*B*,*C4*; $t_{(52)} = 8.193$; $p < 0.001$) or unperturbed slices ($t_{(104)} = 5.018$; $p < 0.001$), slices exposed to NE alone ($t_{(104)} = 5.637$; $p < 0.001$), and slices exposed to AIH ($t_{(104)} = 4.318$; $p < 0.001$; interaction of treatment × time, $F_{(4,52)} = 12.31$; $p < 0.001$; Fig. 1*C4*). The increased IS observed after AIH and NE was attributable to the alternating activation of small and large integrated population bursts. Small and large burst typically alternated in an unpredictable manner.

To test for a dose–response effect, we used twice the concentration of NE (4 μM, $n = 6$) in an additional set of experiments. The effects of the higher dose were similar to the smaller dose of NE when applied during AIH regarding the respiratory frequency and $IS_{amp}$. At 30 min after hypoxic exposure, we observed an increase in the instantaneous frequency of the fictive inspiratory bursts when compared with baseline (Fig. 1*C1*; $t_{(52)} = 3.958$; $p < 0.001$), or, at the same time, unperturbed slices ($t_{(104)} = 3.183$; $p < 0.05$), and slices exposed to NE alone ($t_{(104)} = 2.930$; $p < 0.05$). Besides, the $IS_{amp}$ of the fictive inspiratory bursts increased when compared with baseline (Fig. 1*C4*; $t_{(52)} = 5.990$; $p < 0.001$), or, at the same time, unperturbed slices ($t_{(104)} = 5.535$; $p < 0.001$), slices exposed to NE alone ($t_{(104)} = 5.935$; $p < 0.001$), and slices exposed to AIH ($t_{(104)} = 4.805$; $p < 0.001$). However, neither the instantaneous frequency nor the $IS_{amp}$ were significantly different when compared with slices exposed to AIH and NE at 2 μM. Interestingly, when applied at 4 μM during AIH, NE caused a significant increase in the irregularity of the inspiratory frequency ($IS_{Fr}$; Fig. 1*C2*) when compared with unperturbed slices ($t_{(104)} = 4.094$; $p < 0.001$), slices exposed to NE alone ($t_{(104)} = 3.378$; $p < 0.01$), slices exposed to AIH ($t_{(104)} = 3.534$; $p < 0.01$), and slices exposed to AIH and NE at 2 μM ($t_{(104)} = 3.196$; $p < 0.05$) at the same time. However, the higher dose of NE when applied during AIH also decreased the rhythm amplitude dramatically compared with baseline (Fig. 1*C3*; $t_{(52)} = 3.154$; $p < 0.05$). In two of six cases, the rhythm became so erratic that it became difficult to distinguish rhythmic activity from noise.

In another set of experiments, we applied NE after the AIH exposure to test whether elevated levels of NE during AIH are

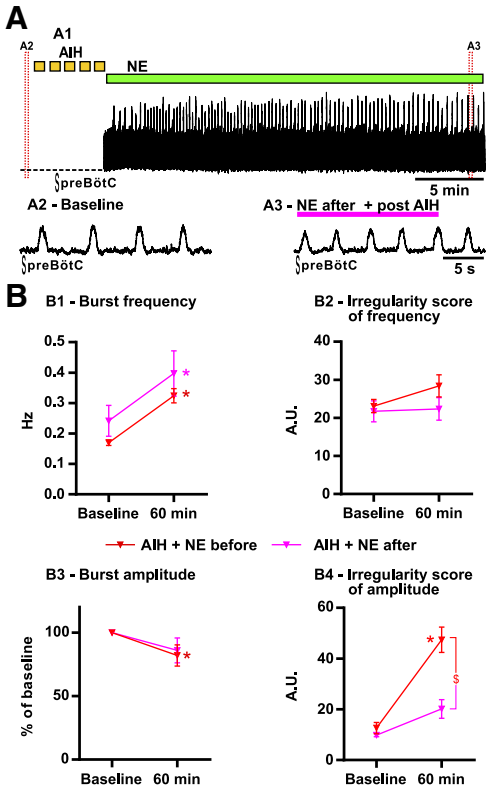


**Figure 2.** Consequences of delayed NE application on the fictive breathing activity recorded from brainstem slices exposed to AIH *in vitro*. ***A***, NE (2 $\mu$M) is applied after the last bout of hypoxia. ***A1*** shows the integrated activity recorded from the preBötC after the last hypoxic bout of AIH. Enlarged timescale of the fictive breathing activity before (***A2***, Baseline) and 30 min after (***A3***) AIH in the presence of NE. ***B***, Parameters of the fictive breathing activity observed before AIH (baseline) and 30 min after the last bout of hypoxia (or 60 min after baseline). The inspiratory burst instantaneous frequency (***B1***) and amplitude (***B3***) as well as the IS of frequency (***B2***) and amplitude (***B4***) were measured (number of slices in each condition: $n = 19$ AIH + NE before; $n = 7$ AIH + NE after). Note the significant decrease of the IS of amplitude in slices in which NE was applied after AIH compared with slices exposed to NE before AIH (two-way ANOVA followed by Holm–Sidak *post hoc* test; * represents significant difference compared with baseline in one group; $ represents significant difference between groups at the same time; different levels of statistical differences are not represented).

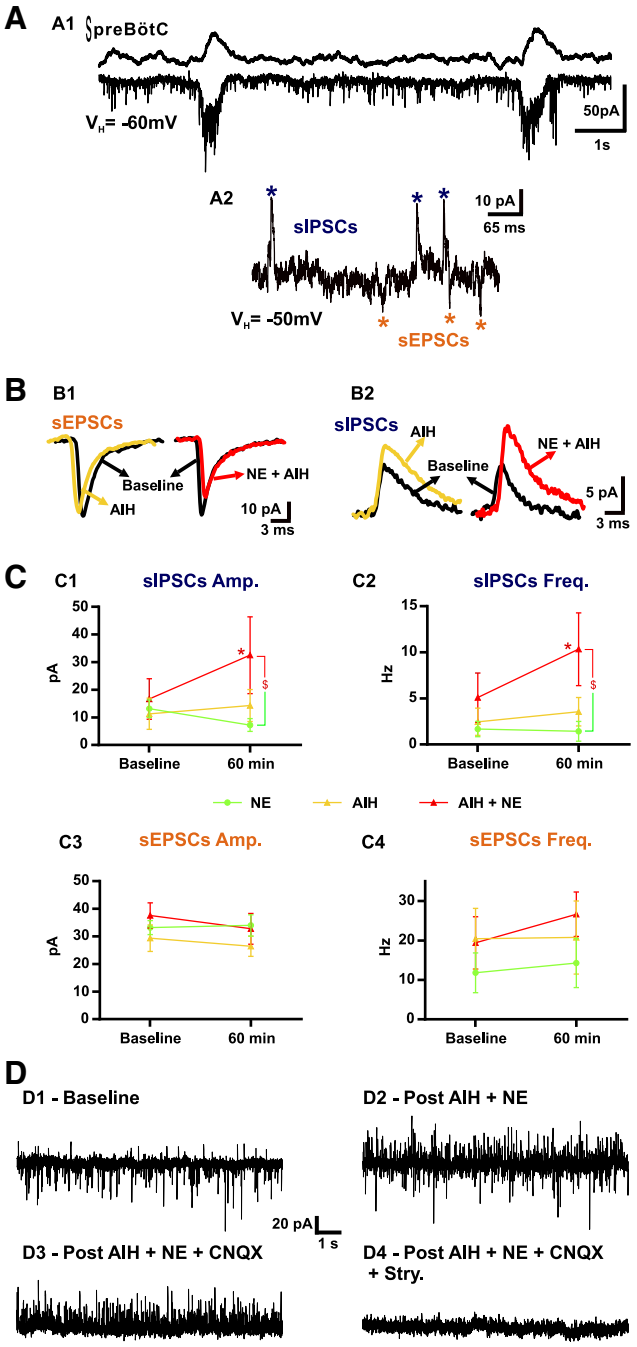


**Figure 3.** Intracellular whole-cell recordings of inspiratory neurons from the preBötC in brainstem slices *in vitro*. ***A***, Example of an inspiratory neuron (bottom trace) in-phase with the fictive breathing activity (top trace) recorded from the preBötC. The neuron is held at a potential of −60 mV ($V_H$) to identify its pattern of activity (***A1***). Then the $V_H$ is raised to −50 mV (***A2***) to allow for better recognition of sIPSCs (blue asterisks) and sEPSCs (orange asterisks). ***B*** shows the average of at least 50 sEPSCs (***B1***) and 50 sIPSCs (***B2***) from one inspiratory neuron before (baseline, black trace) and after (yellow trace) AIH and from another inspiratory neuron before (baseline, black trace) and after (red trace) AIH and NE. ***C*** represents the values of the sIPSC amplitude (***C1***) and frequency (***C2***) and the sEPSC amplitude (***C3***) and frequency (***C4***) under baseline and 30 min after the last bout of hypoxia (or 60 min after baseline). Note the significant increase in sIPSC amplitude and frequency after AIH and NE. ***D*** shows an example of the recording of an inspiratory neuron ($V_H = -50$ mV) before (***D1***, Baseline) and after (***D2***) AIH plus NE exposure. Note that, in the same neuron, application of CNQX blocks all sEPSCs (***D3***), and then application of strychnine (Stry.) blocks all sIPSCs (***D4***) (number of slices in each condition: $n = 8$ NE; $n = 8$ AIH; $n = 5$ AIH + NE 2 $\mu$M; two-way ANOVA followed by Holm–Sidak *post hoc* test; * represents significant difference compared with baseline in one group; $ represents significant difference between groups at the same time; different levels of statistical differences are not represented).

required to induce the irregularity. NE (2 $\mu$M) was applied either immediately after the last hypoxic bout ($n = 3$) or 20 min later ($n = 4$). Both protocols gave the same results, and data were thus pooled. Under these circumstances, NE no longer significantly increases the $IS_{amp}$ of the fictive inspiratory bursts ($n = 7$; 20.2 ± 3.7) when compared with slices exposed to AIH alone (24.8 ± 3.5). Accordingly, the $IS_{amp}$ of the fictive inspiratory bursts was significantly lower when NE was applied after AIH than when NE was applied during AIH (Fig. 2; $t_{(48)} = 4.110$; $p < 0.001$).

### AIH in the presence of NE enhances inhibitory neurotransmission within the preBötC

As is the case for many networks (Cossart et al., 2005; Trasande and Ramirez, 2007; Lewis and Gonzalez-Burgos, 2008; Koch et al., 2010), the normal functioning of the respiratory network depends on a delicate balance between excitation and inhibition that can be disrupted in many disease states. We hypothesized that this balance could also be modified after AIH in the presence of elevated levels of NE. Therefore, to investigate the mechanisms underlying the change in responsiveness to NE, we used voltage-clamp recordings from inspiratory neurons within the preBötC

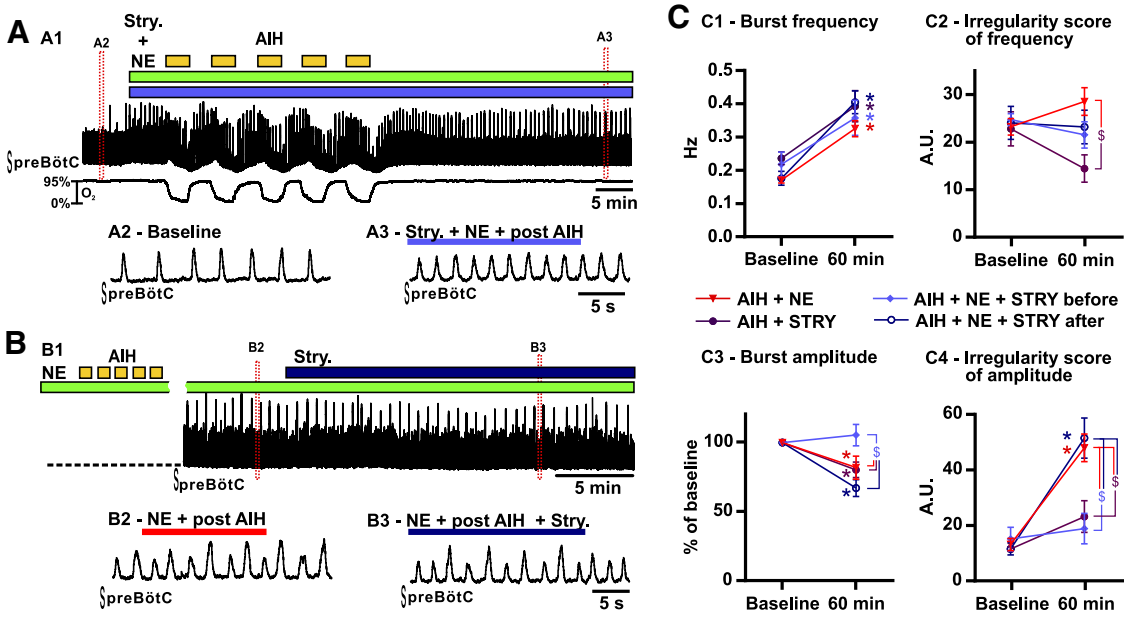


**Figure 4.** Consequences of strychnine (Stry.) coapplication on the fictive breathing activity recorded from brainstem slices exposed to AIH and NE *in vitro*. ***A***, Strychnine is coapplied with NE before AIH exposure. ***A1*** shows the integrated activity recorded from the preBötC (top trace) and the $O_2$ level in the bath (bottom trace). Enlarged timescale of the fictive breathing activity before (***A2***, Baseline) and 30 min after (***A3***) AIH in the presence of NE and Stry. ***B***, Strychnine is applied 30 min after AIH exposure in the presence of NE. ***B1*** shows the integrated activity recorded from the preBötC 30 min after AIH exposure in the presence of NE. Enlarged timescale of the fictive breathing activity before (***B2***) and after (***B3***) strychnine application. ***C***, Parameters of the fictive breathing activity observed before AIH and/or drug injection (baseline) and 30 min after the last bout of hypoxia (or 60 min after baseline). The inspiratory burst instantaneous frequency (***C1***) and amplitude (***C3***) as well as the IS of frequency (***C2***) and amplitude (***C4***) were measured (number of slices in each condition: $n = 19$ AIH + NE; $n = 6$ AIH + Stry.; $n = 6$ AIH + NE + Stry. before; $n = 6$ AIH + NE + Stry. after). Note the significant decrease of the IS of amplitude in slices in which strychnine was coapplied with NE before AIH compared with slices exposed to AIH and NE or strychnine applied after AIH and NE (two-way ANOVA followed by Holm–Sidak *post hoc* test; * represents significant difference compared with baseline in one group; $ represents significant difference between groups at the same time; different levels of statistical differences are not represented).

and characterized the changes in excitatory and inhibitory neurotransmission induced by NE plus AIH.

At a $V_H$ of −50 mV, spontaneous currents recorded in cells clearly exhibit synaptic inward (sEPSCs) and outward (sIPSCs) currents (Fig. 3*A*). We recorded only from one inspiratory neuron per slice, and we repeated the same experimental protocols as those described above for the extracellular recordings. Eight slices were exposed to NE for 70 min, eight slices were exposed to AIH, and five slices were exposed to AIH plus NE. Although all recorded neurons exhibited sEPSCs at a $V_H$ of −50 mV, three neurons (one from the NE group and two from the AIH group) did not exhibit sIPSCs at a $V_H$ of −50 mV and were thus discarded from the analysis of inhibitory currents. At baseline, there was no significant difference between the three groups (Fig. 3*C*). In neurons recorded from slices exposed to AIH plus NE, the amplitude of sIPSCs increased significantly when compared with baseline ($n = 5$; $t_{(15)} = 2.918$; $p < 0.05$) or slices exposed to NE alone ($n = 7$; $t_{(30)} = 2.723$; $p < 0.01$) at the same time, but, although higher, this increase was not significantly different from slices exposed to AIH only ($n = 6$; $t_{(30)} = 1.898$; $p = 0.13$; interaction of treatment × time, $F_{(2,15)} = 3.773$; $p = 0.0471$; Fig. 3*B2*,*C1*). The frequency of sIPSCs increased significantly in neurons recorded from slices exposed to AIH plus NE (Fig. 3*C2*) when compared with baseline ($t_{(15)} = 6.170$; $p < 0.001$) or slices exposed to NE alone ($t_{(30)} = 3.216$; $p < 0.01$) and slices exposed to AIH only ($t_{(30)} = 2.365$; $p < 0.05$) at the same time. In contrast, no significant differences were observed in the changes in sEPSCs amplitude and frequency between slices exposed to NE ($n = 8$), AIH ($n = 8$), or AIH and NE ($n = 5$; Fig. 3*B1*,*C3*,*C4*).

To identify which type of inhibitory synaptic transmission was increased after AIH and NE exposure, we applied strychnine to a subset of cells that were stably recorded for the entire duration of the experimental protocol (Fig. 3*D*). In four of five cells exposed to AIH plus NE, strychnine (1 μM) was applied, resulting in the complete blockade of sIPSCs. Unfortunately, the last cell was lost before the strychnine application. These results strongly suggest that glycinergic transmission was enhanced after AIH plus NE. However, because of our small sample size, we cannot rule out the possibility that GABAergic transmission could also play a role.

### Blockade of inhibition prevents the irregularity induced by AIH and NE *in vitro*

Because AIH and NE specifically increased inhibitory transmission, we hypothesized that blocking inhibition could prevent the irregularity. *In vitro* coapplication of strychnine (1 μM) and NE followed by AIH prevented the irregularity in amplitude ($n = 6$; Fig. 4*A*,*C4*). Indeed, the $IS_{amp}$ did not significantly increase after AIH when compared with baseline ($p = 0.59$) and was significantly reduced compared with slices exposed to AIH and NE (interaction of treatment × time $F_{(3,33)} = 7.483$; $t_{(66)} = 4.202$; $p < 0.001$; Fig. 4*C4*). Interestingly strychnine pretreatment also blocked the reduction of inspiratory burst amplitude caused by AIH and NE ($t_{(66)} = 3.239$; $p < 0.05$; Fig. 4*C3*) However, strychnine pretreatment did not prevent the increase in respiratory frequency (Fig. 4*C1*).

To better determine how NE and AIH interacted with synaptic inhibition, we also applied strychnine alone during AIH ($n = 6$; Fig. 4*C*). Overall, AIH in the presence of strychnine alone caused similar effects on the inspiratory burst frequency, $IS_{Fr}$, and $IS_{amp}$ than AIH in the presence of strychnine combined with NE. In fact, only the inspiratory burst amplitude was maintained significantly higher in the presence of NE. This finding suggests that

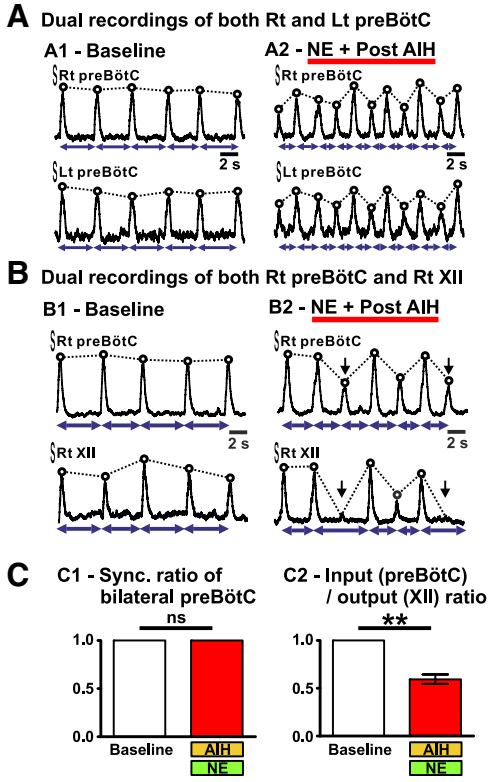


**Figure 5.** Simultaneous recordings of the fictive breathing activity from both the right (Rt) and left (Lt) preBötC or from the XII and the ipsilateral preBötC in brainstem slices *in vitro*. ***A*** shows the integrated activity recorded from both right and left preBötC of one brainstem slice before (***A1***) and after (***A2***) AIH and NE. Note the similar pattern observed on both sides. ***B*** shows the integrated activity recorded from both the right preBötC and the right XII of one brainstem slice before (***B1***) and after (***B2***) AIH and NE. Black arrows indicate inspiratory bursts present on the preBötC but not on the XII after AIH and NE. ***C*** shows the Sync. ratio of bilateral preBötC (***C1***; $n = 5$ slices) and the input/output ratio (***C2***; $n = 5$ slices) before (baseline) and after AIH and NE (paired *t* test; ns, not significant; $^{**}p < 0.01$).

NE increases inhibition during AIH, which then destabilizes the respiratory rhythm. In another set of experiments, we applied strychnine after the appearance of the irregularities *in vitro* ($n = 6$). In this case, strychnine failed to significantly reduce the irregularity of the rhythm (Fig. 4*B*,*C4*). We conclude that blockade of glycinergic inhibition can prevent the AIH-induced change in the responsiveness to NE. Once the AIH-induced alteration in the network configuration is established, it cannot be reversed with strychnine.

### AIH and NE alter the activity recorded from the XII nucleus *in vitro*

To investigate in more detail how the irregularity observed with AIH and NE was manifested in brainstem slices, we recorded simultaneously the activity from the two preBötC (left and right) of slices under the control condition and after exposure to AIH and NE ($n = 5$; Fig. 5*A*). We measured the synchrony (Sync.) of the fictive inspiratory activity present on both left and right preBötC, which we refer to as the Sync. ratio. Under the baseline condition, both preBötC were perfectly synchronized (Sync. ratio = 1; Fig. 5*A1*,*C*). Moreover, dual preBötC recordings revealed the same type of irregularity and pattern after exposure to AIH and NE. Namely, each inspiratory burst present on one preBötC was present on the contralateral preBötC and their shape was similar (Fig. 5*A2*). Therefore, the Sync. ratio value did not change after exposure to AIH and NE (Sync ratio = 1; Fig. 5*C1*).

The population recordings from the preBötC may not necessarily reflect the activity that is also transmitted to the XII motor output (Telgkamp and Ramirez, 1999; St-John et al., 2004). For this reason, we also recorded from the XII. This respiratory motor output is driven by the preBötC in-phase with inspiratory activity. Many research groups use this activity to study fictive breathing in brainstem slices, although the activity in the preBötC is not always identical to the activity recorded from the XII motor output (Telgkamp and Ramirez, 1999). Here, we tested the effect of the exposure to AIH and NE on the XII activity by performing dual recordings from both the preBötC and the ipsilateral XII ($n = 5$; Fig. 5*B*). Under baseline condition, the activity on the XII perfectly matched the activity on the preBötC as measured by an input/output ratio of 1 (i.e., each burst present on the preBötC was always present on the ipsilateral XII). However, after exposure to AIH and NE, the fictive inspiratory output recorded from the XII was significantly altered, because small-amplitude bursts were not always transmitted to the XII (input/output ratio = $0.59 \pm 0.05$, paired *t* test, $t_{(4)} = 7.799$; $p < 0.01$; Fig. 5*B2*,*C2*).

### AIH alters the response of the respiratory network to exogenous NE *in vivo*

The dramatic effect of AIH on the NE response in the isolated *in vitro* network and the fact that small bursts in the *in vitro* network were not reliably transmitted to the respiratory motor output (XII) raised the question whether significant alterations were also seen in the *in vivo* animal. Thus, we performed similar experiments in anesthetized freely breathing mice. We recorded the EMG activity of the inspiratory muscles located in the intercostal space (external intercostal muscles) to assess the inspiratory activity of mice (for details, see Materials and Methods and Fig. 6). In mice exposed to AIH, we measured the blood $SaO_2$. Noteworthy, the blood $O_2$ levels returned to baseline between hypoxic bouts, and repeated pulses caused similar $SaO_2$ desaturation ($34 \pm 10\%$ on the first bout, $37 \pm 10\%$ on the last bout, and an average of $36 \pm 4\%$ for all bouts).

Reminiscent to the *in vitro* situation, exposure to NE was transiently excitatory (Fig. 7*B3*) but had no significant long-term effects: a single bolus of 0.4 $\mu$l of 3 $\mu$M NE ($n = 5$) injected unilaterally into the preBötC area caused no significant changes on amplitude, frequency, and regularity of inspiration when measured 60 min after the injection (Fig. 7*C*). Similarly, saline injection into the preBötC area followed by exposure to AIH ($n = 6$) did not cause significant effects on amplitude, frequency, and regularity (Fig. 7*A*,*C*). AIH alone caused no significant change in the inspiratory frequency confirming that long-term facilitation is not expressed in anesthetized vagus-intact preparations (Janssen and Fregosi, 2000). However, NE injection into the preBötC area followed by exposure to AIH ($n = 8$) had drastic effects on breathing *in vivo* (Fig. 7*B*). NE and AIH significantly increased the irregularity of the inspiratory frequency when compared with baseline ($t_{(16)} = 3.830$; $p < 0.01$) or mice exposed to NE alone ($t_{(32)} = 3.466$; $p < 0.01$) or AIH only ($t_{(32)} = 3.674$; $p < 0.01$; interaction of treatment × time $F_{(2,16)} = 3.690$; $p = 0.0481$; Fig. 7*C2*). *In vivo*, NE and AIH caused no significant change in $IS_{amp}$ compared with other conditions (Fig. 7*C4*).

### AIH alters the response of the respiratory network to endogenous NE *in vivo*

We next tested whether endogenous NE plays a role in the induction of irregularities in the respiratory rhythm observed after AIH *in vivo*. For this purpose, we injected NE reuptake inhibitors into the preBötC area to increase the concentration of NE that is en-

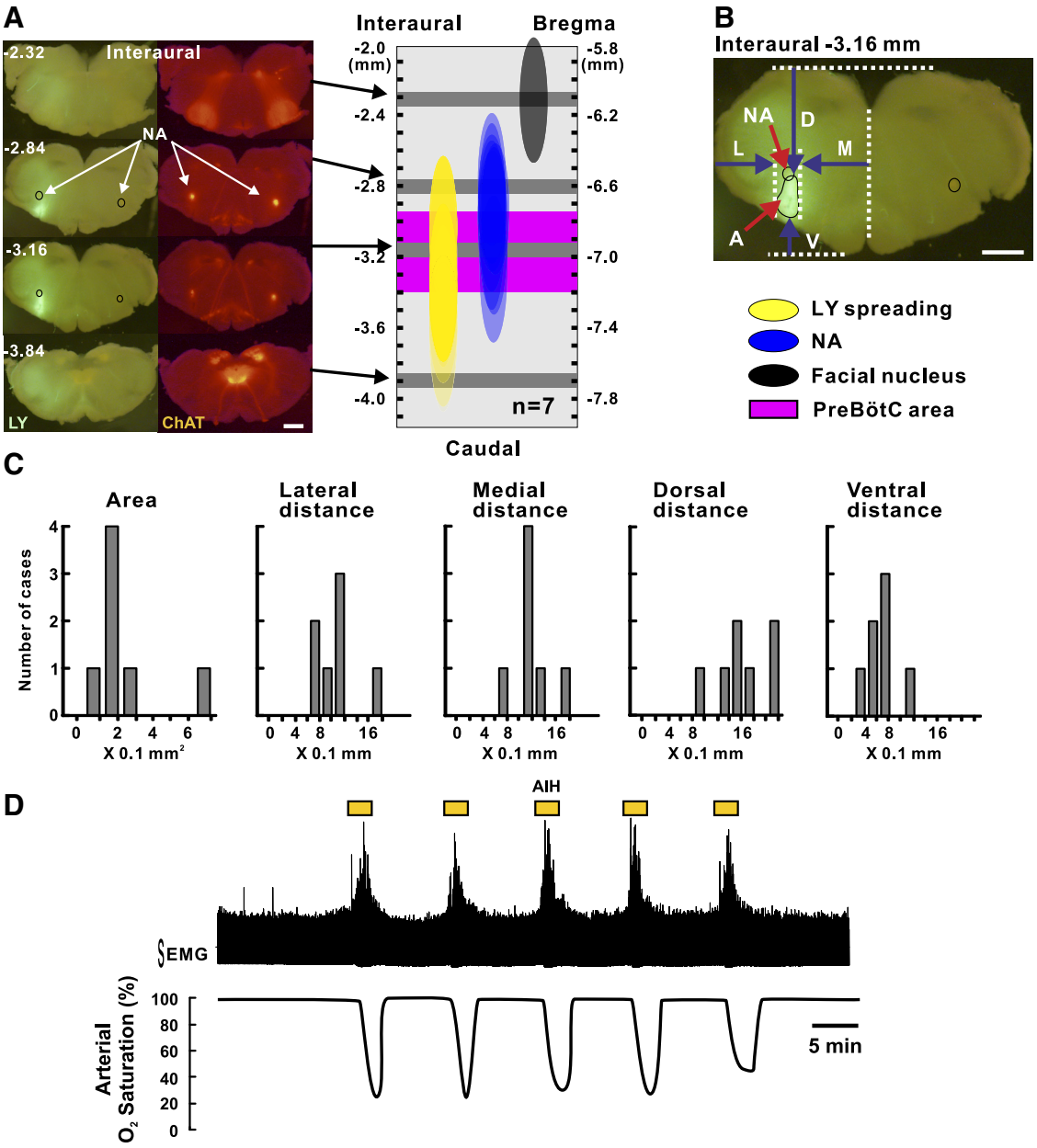


**Figure 6.** Methods for drug injection in the preBötC area and AIH exposure in anesthetized mice *in vivo*. ***A***, The left shows serial sections obtained from the brainstem of a mouse injected with LY (fluorescent green) in the preBötC area (for details, see Materials and Methods). Cholinergic neurons (red fluorescent) are labeled by a fluorescent protein thanks to the genetic construct of the mice (Ai27/ChAT mice) we used in this case. The right shows LY spreading in a reconstructed scheme based on measurements realized in seven injected mice. Note the large overlap between LY staining and preBötC. Scale bar, 1 mm. ***B***, Single section representing the landmarks taken to measure the LY spreading. L, Lateral distance; M, medial distance; D, dorsal distance; V, ventral distance; A, area. Scale bar, 1 mm. ***C***, Histograms showing the LY spreading for each case. ***D*** shows a representative recording of the intercostal muscles EMG integrated activity (top trace) and the corresponding arterial $SaO_2$ monitored using the non-invasive MouseOx system during AIH. Note that the arterial $SaO_2$ drops between 30 and 40% at the end of an isocapnic hypoxic bout (see Materials and Methods).

dogenously released at the synaptic cleft. Thus, a single bolus of 0.4 $\mu$l of desipramine (100 $\mu$M; $n = 15$) or tomoxetine (100 $\mu$M; $n = 13$) was injected unilaterally into the preBötC area. We observed that, in some cases, the respiratory rhythm became so unstable after AIH that the mice ceased breathing and eventually died (Fig. 8*A1*,*B*). Indeed, 53 and 27% of the mice treated with desipramine or tomoxetine, respectively, did not survive after the AIH exposure, whereas none of the mice treated with saline or NE died after AIH exposure (Fig. 8*B*). The respiratory rhythm of the surviving mice treated with desipramine or tomoxetine showed great instability. Similarly to pretreatments with NE, both pretreatments with desipramine or tomoxetine increased the irregularity of the inspiratory frequency (Fig. 8*C*) when compared with baseline ($t_{(18)} = 4.400$, $p < 0.01$ for desipramine and $t_{(18)} = 4.306$, $p < 0.01$ for tomoxetine) or mice exposed to AIH only ($t_{(36)} = 2.703$, $p < 0.01$ for desipramine and $t_{(36)} = 2.496$, $p < 0.01$ for tomoxetine). In addition, pretreatment with desipramine caused a significant increase in $IS_{amp}$ when compared with baseline ($t_{(18)} = 5.893$; $p < 0.001$) or mice exposed to AIH only ($t_{(36)} = 4.006$; $p < 0.001$) and mice exposed to AIH and tomoxetine ($t_{(36)} = 4.242$; $p < 0.001$).

### Blockade of inhibition prevents the irregularity induced by AIH and NE *in vivo*

Because AIH and NE significantly increased inhibitory transmission *in vitro* and because blockade of synaptic inhibition can

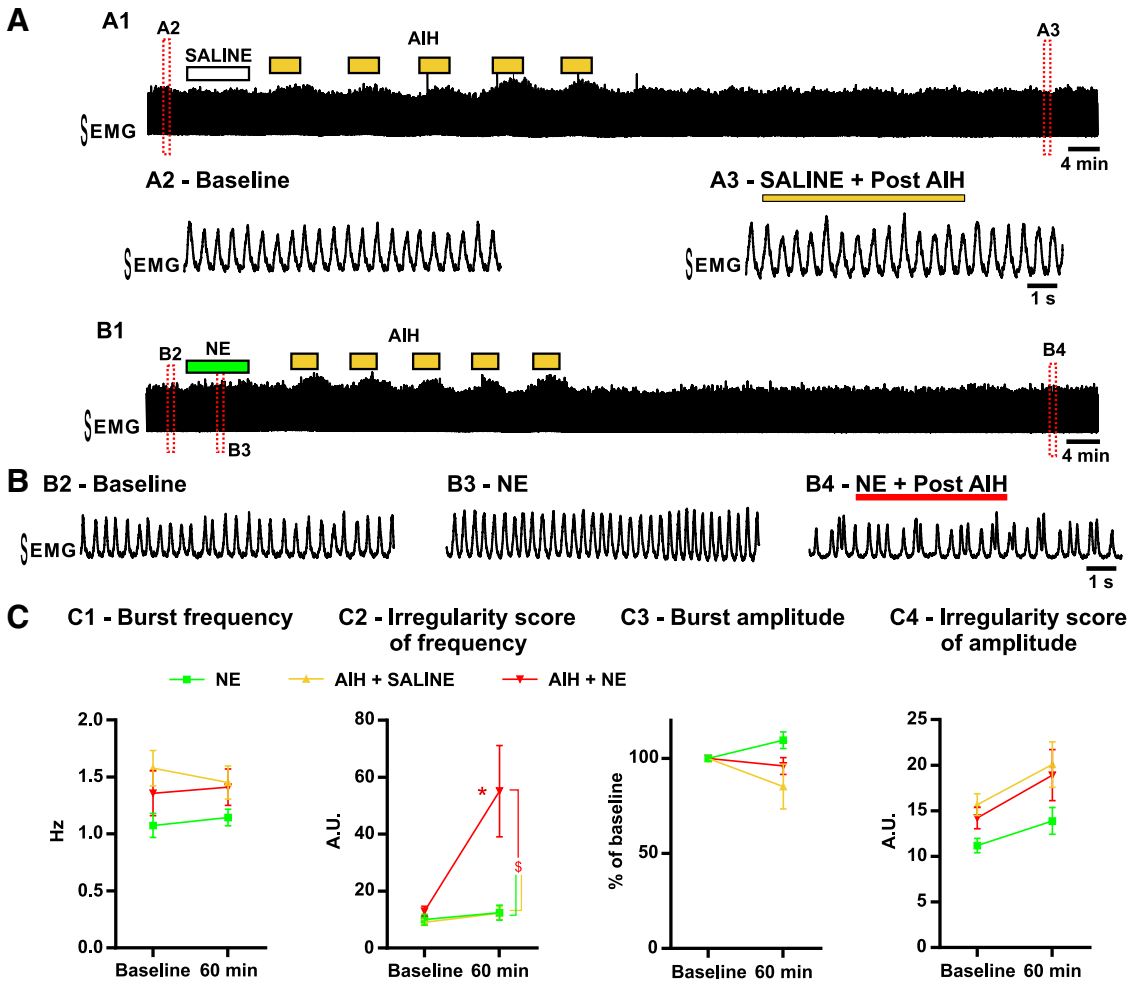


**Figure 7.** The breathing activity is recorded from anesthetized mice *in vivo*. ***A***, Consequences of AIH. ***A1*** shows the EMG integrated activity recorded from the intercostal muscles. Enlarged timescale of the breathing activity before (***A2***, Baseline) and after (***A3***) AIH and saline injection into the preBötC area. ***B***, Same as ***A*** but with NE injection into the preBötC area. ***B1*** shows the EMG integrated activity recorded from the intercostal muscles. Enlarged timescale of the breathing activity before (***B2***, Baseline) and after (***B4***) AIH and NE injection into the preBötC area. Note the transient increase in breathing frequency caused by the NE injection (***B3***). ***C***, Parameters of the breathing activity observed before AIH and/or drug injection (baseline) and 30 min after the last bout of hypoxia (or 60 min after baseline). The burst frequency (***C1***) and amplitude (***C3***) as well as the IS of frequency (***C2***) and amplitude (***C4***) were measured (number of mice in each condition: $n = 5$ NE; $n = 6$ AIH + SALINE; $n = 8$ AIH + NE). Note the significant increase of the IS of frequency in mice exposed to AIH and NE compared with mice exposed to NE alone or AIH and saline (two-way ANOVA followed by Holm–Sidak *post hoc* test; * represents significant difference compared with baseline in one group; $ represents significant difference between groups at the same time; different levels of statistical differences are not represented).

prevent the AIH- and NE-induced irregularity *in vitro*, we hypothesized that blocking the inhibition in the preBötC area could also prevent the irregularity produced by NE and AIH *in vivo*. Therefore, we investigated the effects of blocking glycinergic inhibition in the preBötC area *in vivo*.

Coinjection of strychnine and NE into the preBötC area followed by AIH prevented the breathing irregularity in frequency ($n = 7$; Fig. 9*A*,*C2*). The $IS_{Fr}$ was significantly reduced compared with mice exposed to AIH after injection of NE in the preBötC area ($t_{(34)} = 3.011$; $p < 0.05$; Fig. 9*C2*). Interestingly, strychnine and NE pretreatment followed by AIH exposure also increased the inspiratory burst amplitude when compared with baseline ($t_{(17)} = 3.303$; $p < 0.05$) or mice exposed to AIH and NE ($t_{(34)} = 3.912$; $p < 0.01$) at the same time (Fig. 9*C3*).

In another set of experiments, we applied strychnine after the appearance of the irregularities *in vivo* ($n = 5$). Similar to the situation *in vitro*, this treatment failed to significantly reduce the irregularity of the respiratory rhythm also under *in vivo* conditions (Fig. 9*B3*,*C2*).

### The irregularity induced by AIH and NE *in vitro* is caused by activation of α2-adrenergic receptors

NE can activate different types of adrenergic receptors. More specifically, it has been shown previously that α2-adrenergic receptors in the preBötC area are activated by endogenous release of NE, and, together with α1-adrenergic receptors, the activation of these receptor subtypes plays a critical role in different aspects of respiratory rhythm generation (Viemari and Ramirez, 2006; Zanella et al., 2006; Corcoran and Milsom, 2009; Viemari et al., 2011; Abbott et al., 2013).

In a first set of experiments, we tested the role of α1-adrenergic receptor activation during AIH (Fig. 10*A*,*C*). The application of cirazoline (5 μM; $n = 6$), a selective agonist of α1-adrenergic receptors, during AIH did not cause the same irregularity as NE. Indeed, the $IS_{amp}$ after AIH in the presence of cirazoline was not significantly different from the $IS_{amp}$ after AIH alone ($t_{(74)} = 0.48$; $p = 0.63$) and was significantly reduced compared with the $IS_{amp}$ of slices exposed to AIH and NE ($t_{(74)} = 3.99$; $p < 0.001$).

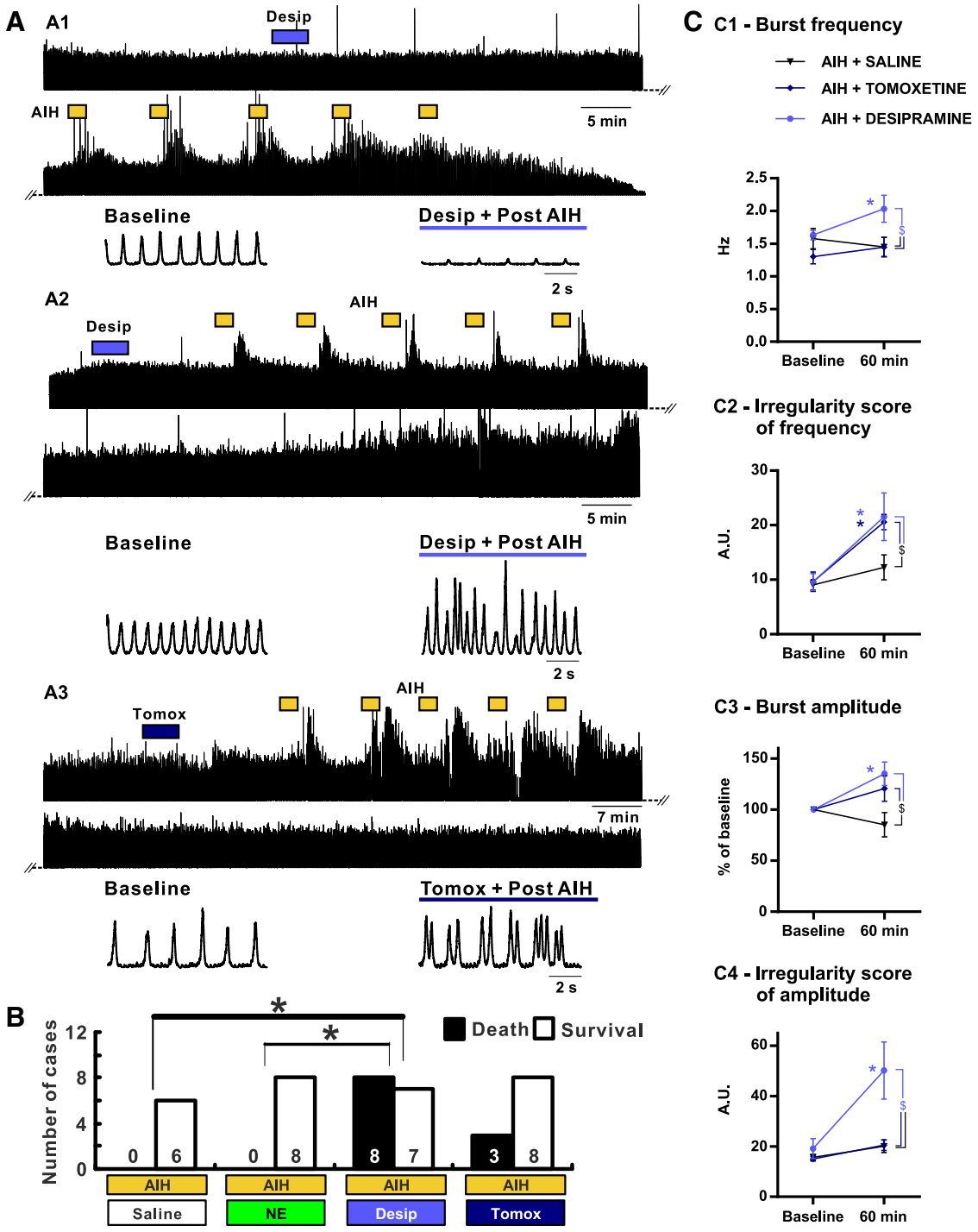


**Figure 8.** Consequences of NE reuptake inhibitors injection in the preBötC area on the breathing activity recorded from anesthetized mice exposed to AIH *in vivo*. ***A***, Desipramine (Desip.) or tomoxetine (Tomox.) is injected into the preBötC area before AIH exposure. ***A1*** shows the EMG integrated activity recorded from the intercostal muscles of a mouse that died after AIH. ***A2*** shows the integrated intercostal EMG activity of a mouse that survived after desipramine injection followed by AIH. Note the irregularity of both the frequency and the amplitude of the respiratory rhythm. ***A3*** shows the integrated intercostal EMG activity after tomoxetine injection followed by AIH. Note the irregularity of the frequency of the respiratory rhythm. ***B***, Histograms showing the number of cases of survival versus death after AIH depending on the drug injected into the preBötC area. Note the poor survival rate when desipramine is injected before AIH. ***C***, Parameters of the breathing activity observed before AIH and/or drug injection (baseline) and 30 min after the last bout of hypoxia (60 min after baseline). The burst frequency (***C1***) and amplitude (***C3***) as well as the IS of frequency (***C2***) and amplitude (***C4***) were measured (number of mice in each condition: $n = 6$ AIH + SALINE; $n = 8$ AIH + TOMOXETINE; $n = 7$ AIH + DESIPRAMINE). Note the significant increase of the IS of frequency in mice in which desipramine or tomoxetine was injected before AIH compared with mice exposed to AIH and saline (two-way ANOVA followed by Holm–Sidak *post hoc* test; * represents significant difference compared with baseline in one group; $ represents significant difference between groups at the same time; a $\chi^2$ test was used to compare the survival rate; different levels of statistical differences are not represented).

To test the role of endogenously activated $\alpha$2-adrenergic receptors in slices, we performed experiments using two different antagonists for $\alpha$2-adrenergic receptors ($n = 3$ with yohimbine at 5 $\mu$M and $n = 3$ with RX821002 [1*H*-imidazole, 2-(2,3-dihydro-2-methoxy-1,4-benzodioxin-2-yl)-4,5-dihydro-1*H*-imidazole hydrochloride at 5 $\mu$M; Fig. 10*B1*,*B2*,*C*). The two antagonists caused similar effects, and the data were thus pooled. Although slightly lower, the $IS_{amp}$ was not significantly different after AIH

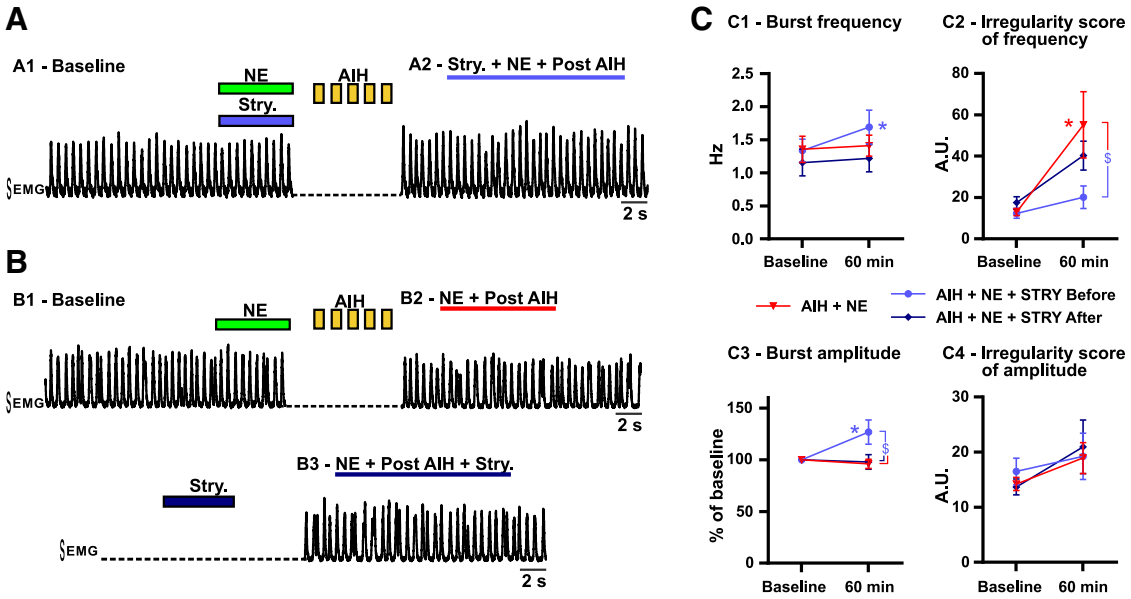


**Figure 9.** Consequences of strychnine (Stry.) coapplication on the breathing activity recorded from anesthetized mice exposed to AIH and NE *in vivo*. ***A***, Strychnine is coinjected with NE into the preBötC area before AIH exposure. ***A1*** shows the EMG integrated activity recorded from the intercostal muscles before AIH exposure (baseline). ***A2*** shows the same EMG integrated activity 30 min after AIH exposure. ***B***, Strychnine is applied 30 min after AIH and NE exposure. The EMG integrated activity recorded from the intercostal muscles is shown before (***B1***), 30 min after AIH and NE injection into the preBötC area (***B2***) and in the same animal after strychnine injection (***B3***). ***C***, Parameters of the breathing activity observed before AIH and/or drug injection (baseline) and 30 min after the last bout of hypoxia (60 min after baseline). The burst frequency (***C1***) and amplitude (***C3***) as well as the IS of frequency (***C2***) and amplitude (***C4***) were measured (number of mice in each condition: $n = 8$ AIH + NE; $n = 7$ AIH + NE + Stry. before; $n = 5$ AIH + NE + Stry. after). Note the significant decrease of the IS of frequency in mice in which strychnine was coapplied with NE before AIH compared with mice exposed to AIH and NE or strychnine applied after AIH and NE (two-way ANOVA followed by Holm–Sidak *post hoc* test; * represents significant difference compared with baseline in one group; $ represents significant difference between groups at the same time; different levels of statistical differences are not represented).

in the presence of NE antagonists (20.4 ± 4.6) when compared with AIH alone (24.8 ± 3.5; $t_{(74)} = 0.68$; $p = 0.49$).

In a last set of experiments, we coapplied NE with either yohimbine (5 $\mu$M; $n = 4$) or RX821002 (5 $\mu$M; $n = 4$) followed by AIH to block the $\alpha$2-adrenergic receptors only (Fig. 10*B3*,*B4*,*C*). The two protocols yielded similar results, and the data were pooled. Interestingly, after blockade of $\alpha$2-adrenergic receptors, NE did not cause an increase of $IS_{amp}$ comparable with the application of NE during AIH ($t_{(78)} = 4.028$; $p < 0.001$). Together, these results suggest that the irregularity induced by NE and AIH is likely attributable to NE acting on $\alpha$2-adrenergic receptors.

## Discussion

NE modulates respiratory rhythmic activity in both the preBötC (Viemari and Ramirez, 2006; Zanella et al., 2006; Corcoran and Milsom, 2009; Viemari et al., 2011; Abbott et al., 2013) and the XII (Parkis et al., 1995; Rukhadze and Kubin, 2007). Under control conditions, stable respiratory rhythmic activity is generated in the presence of NE. However, the same neuromodulator paired with five hypoxic bouts renders the respiratory network irregular. Amplitude irregularities in the preBötC lead to an incomplete transmission of inspiratory bursts to the XII in transverse slice preparations. Consequently, the XII skipped respiratory cycles, resulting in apneas at the level of the XII. This finding is potentially relevant for sleep apnea. The XII innervates the tongue muscles that are activated during breathing to enlarge and stiffen the upper airways, which avoids pharyngeal collapse during wakefulness and sleep (Horner, 1996; Bailey et al., 2006). After AIH and NE, the phasic activation of the XII fails during some respiratory cycles. If respiratory activity is maintained in the phrenic nerve, this could lead to a mismatch in the activation of diaphragm and upper airways, the buildup of negative pressure, and pharyngeal collapse, which could contribute to obstructive sleep apnea (Ramirez et al., 2013a).

Interestingly, NE injected into the preBötC and paired with AIH resulted in dramatic frequency irregularities in the ventilatory motor output of freely breathing animals. Thus, the amplitude irregularities generated at the level of the respiratory rhythm-generating network could be translated into the frequency irregularities in the freely breathing animals. This is plausible because the same area (preBötC) was exposed to NE *in vivo* and *in vitro*. However, other mechanisms may contribute to the *in vivo* phenomenon when compared with a reduced preparation *in vitro*.

We identified a potential cellular mechanism for these irregularities. AIH paired with NE enhanced synaptic inhibition within the preBötC. This synaptic effect seems to be causally related to the irregularities, because blocking glycinergic inhibition within the preBötC prevented the occurrence of irregularities *in vitro* and *in vivo*. We hypothesize that the increased inhibition contributes to the decreased drive to the XII, which is normally under the influence of both excitatory and inhibitory inputs. This unbalance may uncouple the XII activity from the respiratory rhythm-generating network as suggested by others (St-John et al., 2004). The synaptic inhibition likely included neurons located within the respiratory slice. Glycinergic neurons are present within the preBötC (Shao and Feldman, 1997) and may account for half of the neurons in this area (Winter et al., 2009, 2010). They are well inserted inside the respiratory rhythm-generating network, with some being tonically active during expiration or in-phase with inspiration and some having bursting pacemaker properties (Winter et al., 2009; Morgado-Valle et al., 2010; Koizumi et al., 2013). These neurons may play an impor-

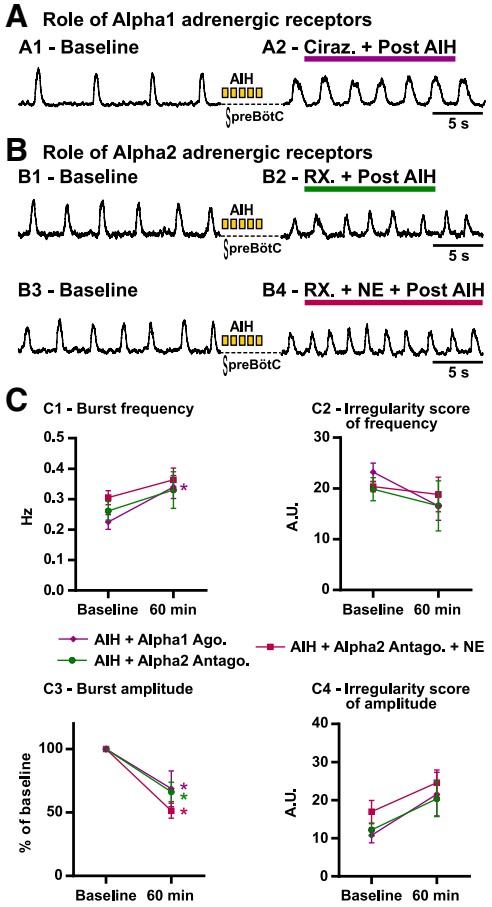


**Figure 10.** Role of $\alpha$1- and $\alpha$2-adrenergic receptors in the irregularity induced by AIH and NE *in vitro*. ***A***, The $\alpha$1-adrenergic receptor agonist cirazoline (ciraz., 5 $\mu$M) is applied during AIH. ***A1*** shows the integrated activity recorded from the preBötC before (baseline) and 30 min after (***A2***) AIH in the presence of cirazoline. ***B*** shows the effect of $\alpha$2-adrenergic receptor blockade during AIH with or without NE coapplication. The integrated activity is recorded from the preBötC before (***B1***, Baseline) and 30 min after AIH (***B2***) in the presence of RX821002 (RX., 5 $\mu$M). Similarly, the integrated activity is recorded from the preBötC before (***B3***, Baseline) and 30 min after AIH (***B4***) in the presence of RX821002 and NE. ***C***, Parameters of the fictive breathing activity observed before AIH (baseline) and 30 min after the last bout of hypoxia (or 60 min after baseline). The inspiratory burst instantaneous frequency (***C1***) and amplitude (***C3***) as well as the IS of frequency (***C2***) and amplitude (***C4***) were measured (number of slices in each condition: $n = 6$ Alpha1 Ago. + AIH.; $n = 6$ Alpha2 Antago.; $n = 8$ Alpha2 Antago. + AIH). Note that the irregularity of inspiratory burst amplitude observed with AIH and NE is not present when $\alpha$2-adrenergic receptors are not activated (two-way ANOVA followed by Holm–Sidak *post hoc* test; * represents significant difference compared with baseline in one group; different levels of statistical differences are not represented).

tant role in modulating and stabilizing the respiratory rhythm (Ramirez et al., 2011). Interestingly, the presence of NE during AIH was required to produce the irregularities, and, once the respiratory network assumed this state, the irregularities persisted and were not reversed by the blockade of synaptic inhibition. Thus, it is not simply the increased synaptic inhibition that alters the responsiveness of the network to NE. Rather, the presence of synaptic inhibition promotes a network state that, once assumed, develops irregularity in the presence of NE.

Glycinergic inhibition is involved in the hypoxic response (Ramirez et al., 1998a; Kato et al., 2000; St-John and Leiter, 2002). However, long-term effects of a single hypoxia bout have not been studied and may be different from the long-term effects of AIH. Long-term synaptic changes, such as LTP and LTD, are well known plasticity mechanisms (Hunt and Castillo, 2012; Lisman et al., 2012) that are also closely regulated by neuromodulation (Han et al., 2012; Huang et al., 2012). Another important mechanism in which long-term synaptic changes regulate neuronal network states is homeostatic plasticity (Garcia et al., 2011; Turrigiano, 2011; Spitzer, 2012). Homeostatic plasticity exists at the level of the nucleus tractus solitarius (NTS) in rats (Kline et al., 2007). After exposure to chronic intermittent hypoxia, the augmentation of spontaneous presynaptic transmitter release causes an increase in NTS postsynaptic cell activity counterbalanced by a reduction in evoked synaptic transmission between sensory afferents and NTS postsynaptic cells. Although most long-term plasticity studies have focused on the physiological role of synaptic mechanisms in maintaining regular activity, increased evidence reveal that synaptic plasticity can drive neuropathological conditions, such as epilepsy (Trasande and Ramirez, 2007; Koch et al., 2010). Our study can be considered as another example in which long-term changes in synaptic inhibition result in a network configuration that promotes irregularities.

Although comparisons between species are associated with numerous caveats, our findings could be relevant for clinical conditions associated with episodic hypoxia (Garcia et al., 2013; Ramirez et al., 2013a). Indeed, we exposed mice to AIH, which led to severe, yet brief, blood $SaO_2$ (<40–50%) reminiscent of levels reached during severe apneas. In patients suffering from obstructive sleep apneas, polysomnographic recordings revealed dramatic drops in $SaO_2$ (<80–70%) occurring >30 times/h (Edwards et al., 2010; Edwards and White, 2011; Leung et al., 2012). In healthy preterm infants, a higher apnea frequency during sleep has been reported (Silvestri et al., 2002; Hunt et al., 2011; Vagedes et al., 2013), causing intermittent hypoxemia ($SaO_2$ < 80%). Interestingly, we used an acute stimulation while repeated oxygen desaturations occur chronically in most of these diseases. For instance, recurrent apneas persist for several weeks in preterm infants (Poets et al., 1991; Eichenwald et al., 1997). Thus, it would be interesting to test our hypothesis on mice exposed to chronic intermittent hypoxia.

Our study is also significant for patients with Rett syndrome suffering from frequent apneas (>10 s; $SaO_2$ < 80%) during wakefulness (Weese-Mayer et al., 2008; Ramirez et al., 2013b). In the most severe cases, $SaO_2$ falls below 50% during long-lasting apneas (Southall et al., 1988; Julu et al., 2001). Besides, mouse models mutated for the responsible gene *Mecp2* (Guy et al., 2001; Katz et al., 2009) have deficiencies in bioaminergic neuromodulation. Specifically, the number of tyrosine hydroxylase-positive medullary neurons, NE, and serotonin concentrations are lower (Viemari et al., 2005; Samaco et al., 2009; Taneja et al., 2009; Zhang et al., 2010a; Panayotis et al., 2011). Several human studies confirmed this deficiency in monoaminergic systems (Zoghbi et al., 1985; Brücke et al., 1987; Lekman et al., 1989; Paterson et al., 2005; Samaco et al., 2009). The obvious hypothesis is that the NE decrease causes the breathing irregularities, a hypothesis that was tested by increasing NE levels in the synaptic cleft in *Mecp2*-deficient mice (Roux et al., 2007; Zanella et al., 2008). Although the lifespan of these mice was extended, mice eventually developed breathing irregularities and died. Thus, the known modulatory deficiency cannot fully explain the respiratory dysfunction in *Mecp2*-deficient mice and patients with Rett syndrome. Moreover, breathing in these patients is more irregular and apneas more prominent during wakefulness (Weese-Mayer et al., 2008), a state during which NE levels and NE neuron discharges are elevated. In the locus ceruleus, the activity of NE neurons is high during wakefulness, decreases during non-rapid eye movement (REM) sleep, and stops during REM sleep (Aston-Jones and

Bloom, 1981; Saper et al., 2010; Takahashi et al., 2010). Similarly the NE drive to XII is high in wakefulness, decreases in non-REM sleep, and is minimal in REM sleep (Fenik et al., 2005; Chan et al., 2006). Although it is tempting to speculate that the hypoxic episodes have caused these irregularities as NE increases in wakefulness, such an argument is difficult to make for a human condition. In mice, *Mecp2* mutations have been associated with an imbalance in excitatory and inhibitory transmission. The focus has been on a dysregulation of GABAergic synaptic mechanisms, but GABAergic transmission can be enhanced and reduced in different regions or states of the brain (Dani et al., 2005; Medrihan et al., 2008; Chao et al., 2010; Zhang et al., 2010b). The characterization of synaptic inhibition in respiratory neurons of *Mecp2*-deficient mice remains to be performed to determine whether chronic intermittent hypoxia in patients with Rett syndrome contributes to this dysregulation in states of elevated NE.

It is known that AIH causes prolonged increases in frequency and amplitude of motor output in rodents (Hayashi et al., 1993; Baker and Mitchell, 2000). The likely site for long-term frequency modulation is the preBötC (Blitz and Ramirez, 2002). AIH causes also immediate changes in the modulatory milieu (Bach and Mitchell, 1996; Kinkead and Mitchell, 1999), the production of reactive oxygen species (ROS) (MacFarlane and Mitchell, 2009; Pawar et al., 2009), long-term changes involving gene expression, and an ROS-activated PKC pathway causing BDNF synthesis and increased glutamatergic synaptic transmission (Baker-Herman et al., 2004). Although previous studies characterized the effects of AIH on synaptic mechanisms, it is likely that the observed increase in synaptic inhibition involves some of these mechanisms.

What makes this study conceptually novel is the finding that the AIH-induced changes lead to fundamental differences in noradrenergic modulation. Based on our study, one cannot assume that a given neuromodulator has similar effects in a normal network when compared with one that was exposed to intermittent hypoxia. Given that many neuromodulators are used clinically, their effectiveness may be fundamentally different in patients presenting with sleep apnea or other disorders.

## References


Abbott SB, DePuy SD, Nguyen T, Coates MB, Stornetta RL, Guyenet PG (2013) Selective optogenetic activation of rostral ventrolateral medullary catecholaminergic neurons produces cardiorespiratory stimulation in conscious mice. J Neurosci 33:3164–3177. CrossRef Medline

Armstrong CM, Gilly WF (1992) Access resistance and space clamp problems associated with whole-cell patch clamping. Methods Enzymol 207:100–122. CrossRef Medline

Aston-Jones G, Bloom FE (1981) Activity of norepinephrine-containing locus coeruleus neurons in behaving rats anticipates fluctuations in the sleep-waking cycle. J Neurosci 1:876–886. Medline

Bach KB, Mitchell GS (1996) Hypoxia-induced long-term facilitation of respiratory activity is serotonin dependent. Respir Physiol 104:251–260. CrossRef Medline

Bailey EF, Huang YH, Fregosi RF (2006) Anatomic consequences of intrinsic tongue muscle activation. J Appl Physiol 101:1377–1385. CrossRef Medline

Baker TL, Mitchell GS (2000) Episodic but not continuous hypoxia elicits long-term facilitation of phrenic motor output in rats. J Physiol 529:215–219. CrossRef Medline

Baker-Herman TL, Mitchell GS (2002) Phrenic long-term facilitation requires spinal serotonin receptor activation and protein synthesis. J Neurosci 22:6239–6246. Medline

Baker-Herman TL, Fuller DD, Bavis RW, Zabka AG, Golder FJ, Doperalski NJ, Johnson RA, Watters JJ, Mitchell GS (2004) BDNF is necessary and sufficient for spinal respiratory plasticity following intermittent hypoxia. Nat Neurosci 7:48–55. CrossRef Medline

Barthe JY, Clarac F (1997) Modulation of the spinal network for locomotion by substance P in the neonatal rat. Exp Brain Res 115:485–492. CrossRef Medline

Ben-Mabrouk F, Tryba AK (2010) Substance P modulation of TRPC3/7 channels improves respiratory rhythm regularity and ICAN-dependent pacemaker activity. Eur J Neurosci 31:1219–1232. CrossRef Medline

Blanchi B, Sieweke MH (2005) Mutations of brainstem transcription factors and central respiratory disorders. Trends Mol Med 11:23–30. CrossRef Medline

Blitz DM, Ramirez JM (2002) Long-term modulation of respiratory network activity following anoxia in vitro. J Neurophysiol 87:2964–2971. Medline

Bouvier J, Autran S, Dehorter N, Katz DM, Champagnat J, Fortin G, Thoby-Brisson M (2008) Brain-derived neurotrophic factor enhances fetal respiratory rhythm frequency in the mouse preBotzinger complex in vitro. Eur J Neurosci 28:510–520. CrossRef Medline

Brücke T, Sofic E, Killian W, Rett A, Riederer P (1987) Reduced concentrations and increased metabolism of biogenic amines in a single case of Rett-syndrome: a postmortem brain study. J Neural Transm 68:315–324. CrossRef Medline

Burnstock G, Krügel U, Abbracchio MP, Illes P (2011) Purinergic signalling: from normal behaviour to pathological brain function. Prog Neurobiol 95:229–274. CrossRef Medline

Caiazzo M, Dell'Anno MT, Dvoretskova E, Lazarevic D, Taverna S, Leo D, Sotnikova TD, Menegon A, Roncaglia P, Colciago G, Russo G, Carninci P, Pezzoli G, Gainetdinov RR, Gustincich S, Dityatev A, Broccoli V (2011) Direct generation of functional dopaminergic neurons from mouse and human fibroblasts. Nature 476:224–227. CrossRef Medline

Chan E, Steenland HW, Liu H, Horner RL (2006) Endogenous excitatory drive modulating respiratory muscle activity across sleep-wake states. Am J Respir Crit Care Med 174:1264–1273. CrossRef Medline

Chao HT, Chen H, Samaco RC, Xue M, Chahrour M, Yoo J, Neul JL, Gong S, Lu HC, Heintz N, Ekker M, Rubenstein JL, Noebels JL, Rosenmund C, Zoghbi HY (2010) Dysfunction in GABA signalling mediates autism-like stereotypies and Rett syndrome phenotypes. Nature 468:263–269. CrossRef Medline

Corcoran AE, Milsom WK (2009) Maturational changes in pontine and medullary alpha-adrenoceptor influences on respiratory rhythm generation in neonatal rats. Respir Physiol Neurobiol 165:195–201. CrossRef Medline

Cossart R, Bernard C, Ben-Ari Y (2005) Multiple facets of GABAergic neurons and synapses: multiple fates of GABA signalling in epilepsies. Trends Neurosci 28:108–115. CrossRef Medline

Dani VS, Chang Q, Maffei A, Turrigiano GG, Jaenisch R, Nelson SB (2005) Reduced cortical activity due to a shift in the balance between excitation and inhibition in a mouse model of Rett syndrome. Proc Natl Acad Sci U S A 102:12560–12565. CrossRef Medline

Doi A, Ramirez JM (2008) Neuromodulation and the orchestration of the respiratory rhythm. Respir Physiol Neurobiol 164:96–104. CrossRef Medline

Doi A, Ramirez JM (2010) State-dependent interactions between excitatory neuromodulators in the control of breathing. J Neurosci 30:8251–8262. CrossRef Medline

Edwards BA, White DP (2011) Control of the pharyngeal musculature during wakefulness and sleep: implications in normal controls and sleep apnea. Head Neck 33 [Suppl 1]:S37–S45. CrossRef

Edwards BA, O'Driscoll DM, Ali A, Jordan AS, Trinder J, Malhotra A (2010) Aging and sleep: physiology and pathophysiology. Semin Respir Crit Care Med 31:618–633. CrossRef Medline

Eichenwald EC, Aina A, Stark AR (1997) Apnea frequently persists beyond term gestation in infants delivered at 24 to 28 weeks. Pediatrics 100:354–359. CrossRef Medline

Ellenberger HH, Feldman JL, Zhan WZ (1990) Subnuclear organization of the lateral tegmental field of the rat. II: catecholamine neurons and ventral respiratory group. J Comp Neurol 294:212–222. CrossRef Medline

Fenik VB, Davies RO, Kubin L (2005) REM sleep-like atonia of hypoglossal (XII) motoneurons is caused by loss of noradrenergic and serotonergic inputs. Am J Respir Crit Care Med 172:1322–1330. CrossRef Medline

Frederick AL, Stanwood GD (2009) Drugs, biogenic amine targets and the developing brain. Dev Neurosci 31:7–22. CrossRef Medline

Garcia AJ 3rd, Putnam RW, Dean JB (2010) Hyperbaric hyperoxia and normobaric reoxygenation increase excitability and activate oxygen-induced

potentiation in CA1 hippocampal neurons. J Appl Physiol 109:804–819. CrossRef Medline

Garcia AJ 3rd, Zanella S, Koch H, Doi A, Ramirez JM (2011) Chapter 3—networks within networks: the neuronal control of breathing. Prog Brain Res 188:31–50. CrossRef Medline

Garcia AJ 3rd, Koschnitzky JE, Dashevskiy T, Ramirez JM (2013) Cardiorespiratory coupling in health and disease. Auton Neurosci 175:26–37. CrossRef Medline

Gray PA, Janczewski WA, Mellen N, McCrimmon DR, Feldman JL (2001) Normal breathing requires preBotzinger complex neurokinin-1 receptor-expressing neurons. Nat Neurosci 4:927–930. CrossRef Medline

Guy J, Hendrich B, Holmes M, Martin JE, Bird A (2001) A mouse Mecp2-null mutation causes neurological symptoms that mimic Rett syndrome. Nat Genet 27:322–326. CrossRef Medline

Han J, Kesner P, Metna-Laurent M, Duan T, Xu L, Georges F, Koehl M, Abrous DN, Mendizabal-Zubiaga J, Grandes P, Liu Q, Bai G, Wang W, Xiong L, Ren W, Marsicano G, Zhang X (2012) Acute cannabinoids impair working memory through astroglial CB1 receptor modulation of hippocampal LTD. Cell 148:1039–1050. CrossRef Medline

Harris-Warrick RM, Johnson BR (2010) Checks and balances in neuromodulation. Front Behav Neurosci 4:pii: 47. CrossRef Medline

Hart AK, Fioravante D, Liu RY, Phares GA, Cleary LJ, Byrne JH (2011) Serotonin-mediated synapsin expression is necessary for long-term facilitation of the Aplysia sensorimotor synapse. J Neurosci 31:18401–18411. CrossRef Medline

Hasselmo ME, Sarter M (2011) Modes and models of forebrain cholinergic neuromodulation of cognition. Neuropsychopharmacology 36:52–73. CrossRef Medline

Hayashi F, Coles SK, Bach KB, Mitchell GS, McCrimmon DR (1993) Time-dependent phrenic nerve responses to carotid afferent activation: intact vs. decerebellate rats. Am J Physiol 265:R811–R819. Medline

Hill AA, Garcia AJ 3rd, Zanella S, Upadhyaya R, Ramirez JM (2011) Graded reductions in oxygenation evoke graded reconfiguration of the isolated respiratory network. J Neurophysiol 105:625–639. CrossRef Medline

Horner RL (1996) Motor control of the pharyngeal musculature and implications for the pathogenesis of obstructive sleep apnea. Sleep 19:827–853. Medline

Hu JY, Baussi O, Levine A, Chen Y, Schacher S (2011) Persistent long-term synaptic plasticity requires activation of a new signaling pathway by additional stimuli. J Neurosci 31:8841–8850. CrossRef Medline

Huang S, Treviño M, He K, Ardiles A, Pasquale Rd, Guo Y, Palacios A, Huganir R, Kirkwood A (2012) Pull-push neuromodulation of LTP and LTD enables bidirectional experience-induced synaptic scaling in visual cortex. Neuron 73:497–510. CrossRef Medline

Hunt CE, Corwin MJ, Weese-Mayer DE, Ward SL, Ramanathan R, Lister G, Tinsley LR, Heeren T, Rybin D; Collaborative Home Infant Monitoring Evaluation (CHIME) Study Group (2011) Longitudinal assessment of hemoglobin oxygen saturation in preterm and term infants in the first six months of life. J Pediatr 159:377–383.e1. CrossRef Medline

Hunt DL, Castillo PE (2012) Synaptic plasticity of NMDA receptors: mechanisms and functional implications. Curr Opin Neurobiol 22:496–508. CrossRef Medline

Janssen PL, Fregosi RF (2000) No evidence for long-term facilitation after episodic hypoxia in spontaneously breathing, anesthetized rats. J Appl Physiol 89:1345–1351. Medline

Jitsuki S, Takemoto K, Kawasaki T, Tada H, Takahashi A, Becamel C, Sano A, Yuzaki M, Zukin RS, Ziff EB, Kessels HW, Takahashi T (2011) Serotonin mediates cross-modal reorganization of cortical circuits. Neuron 69:780–792. CrossRef Medline

Julu PO, Kerr AM, Apartopoulos F, Al-Rawas S, Engerström IW, Engerström L, Jamal GA, Hansen S (2001) Characterisation of breathing and associated central autonomic dysfunction in the Rett disorder. Arch Dis Child 85:29–37. CrossRef Medline

Kato T, Hayashi F, Tatsumi K, Kuriyama T, Fukuda Y (2000) Inhibitory mechanisms in hypoxic respiratory depression studied in an in vitro preparation. Neurosci Res 38:281–288. CrossRef Medline

Katsnelson A (2011) Experimental therapies for Parkinson's disease: why fake it? Nature 476:142–144. CrossRef Medline

Katz DM, Dutschmann M, Ramirez JM, Hilaire G (2009) Breathing disorders in Rett syndrome: progressive neurochemical dysfunction in the respiratory network after birth. Respir Physiol Neurobiol 168:101–108. CrossRef Medline

Kinkead R, Mitchell GS (1999) Time-dependent hypoxic ventilatory responses in rats: effects of ketanserin and 5-carboxamidotryptamine. Am J Physiol 277:R658–666. Medline

Kline DD, Ramirez-Navarro A, Kunze DL (2007) Adaptive depression in synaptic transmission in the nucleus of the solitary tract after in vivo chronic intermittent hypoxia: evidence for homeostatic plasticity. J Neurosci 27:4663–4673. CrossRef Medline

Kobayashi K (2010) Hippocampal mossy fiber synaptic transmission and its modulation. Vitam Horm 82:65–85. CrossRef Medline

Koch H, Huh SE, Elsen FP, Carroll MS, Hodge RD, Bedogni F, Turner MS, Hevner RF, Ramirez JM (2010) Prostaglandin E2 induced synaptic plasticity in neocortical networks of organotypic slice cultures. J Neurosci 30:11678–11687. CrossRef Medline

Koizumi H, Koshiya N, Chia JX, Cao F, Nugent J, Zhang R, Smith JC (2013) Structural-functional properties of identified excitatory and inhibitory interneurons within pre-Botzinger complex respiratory microcircuits. J Neurosci 33:2994–3009. CrossRef Medline

Kriks S, Shim JW, Piao J, Ganat YM, Wakeman DR, Xie Z, Carrillo-Reid L, Auyeung G, Antonacci C, Buch A, Yang L, Beal MF, Surmeier DJ, Kordower JH, Tabar V, Studer L (2011) Dopamine neurons derived from human ES cells efficiently engraft in animal models of Parkinson's disease. Nature 480:547–551. CrossRef Medline

Krugel LK, Biele G, Mohr PN, Li SC, Heekeren HR (2009) Genetic variation in dopaminergic neuromodulation influences the ability to rapidly and flexibly adapt decisions. Proc Natl Acad Sci U S A 106:17951–17956. CrossRef Medline

Lee YA, Goto Y (2011) Neurodevelopmental disruption of cortico-striatal function caused by degeneration of habenula neurons. PLoS One 6:e19450. CrossRef Medline

Lekman A, Witt-Engerström I, Gottfries J, Hagberg BA, Percy AK, Svennerholm L (1989) Rett syndrome: biogenic amines and metabolites in postmortem brain. Pediatr Neurol 5:357–362. CrossRef Medline

Leung RS, Comondore VR, Ryan CM, Stevens D (2012) Mechanisms of sleep-disordered breathing: causes and consequences. Pflugers Arch 463:213–230. CrossRef Medline

Lewis DA, González-Burgos G (2008) Neuroplasticity of neocortical circuits in schizophrenia. Neuropsychopharmacology 33:141–165. CrossRef Medline

Lieske SP, Thoby-Brisson M, Telgkamp P, Ramirez JM (2000) Reconfiguration of the neural network controlling multiple breathing patterns: eupnea, sighs and gasps. Nat Neurosci 3:600–607. CrossRef Medline

Lisman J, Yasuda R, Raghavachari S (2012) Mechanisms of CaMKII action in long-term potentiation. Nat Rev Neurosci 13:169–182. CrossRef Medline

Lusardi TA (2009) Adenosine neuromodulation and traumatic brain injury. Curr Neuropharmacol 7:228–237. CrossRef Medline

MacFarlane PM, Mitchell GS (2009) Episodic spinal serotonin receptor activation elicits long-lasting phrenic motor facilitation by an NADPH oxidase-dependent mechanism. J Physiol 587:5469–5481. CrossRef Medline

Madisen L, Mao T, Koch H, Zhuo JM, Berenyi A, Fujisawa S, Hsu YW, Garcia AJ 3rd, Gu X, Zanella S, Kidney J, Gu H, Mao Y, Hooks BM, Boyden ES, Buzsáki G, Ramirez JM, Jones AR, Svoboda K, Han X, Turner EE, Zeng H (2012) A toolbox of Cre-dependent optogenetic transgenic mice for light-induced activation and silencing. Nat Neurosci 15:793–802. CrossRef Medline

Medrihan L, Tantalaki E, Aramuni G, Sargsyan V, Dudanova I, Missler M, Zhang W (2008) Early defects of GABAergic synapses in the brain stem of a MeCP2 mouse model of Rett syndrome. J Neurophysiol 99:112–121. CrossRef Medline

Morgado-Valle C, Baca SM, Feldman JL (2010) Glycinergic pacemaker neurons in preBotzinger complex of neonatal mouse. J Neurosci 30:3634–3639. CrossRef Medline

Panayotis N, Ghata A, Villard L, Roux JC (2011) Biogenic amines and their metabolites are differentially affected in the Mecp2-deficient mouse brain. BMC Neurosci 12:47. CrossRef Medline

Parkis MA, Bayliss DA, Berger AJ (1995) Actions of norepinephrine on rat hypoglossal motoneurons. J Neurophysiol 74:1911–1919. Medline

Paterson DS, Thompson EG, Belliveau RA, Antalffy BA, Trachtenberg FL, Armstrong DD, Kinney HC (2005) Serotonin transporter abnormality in the dorsal motor nucleus of the vagus in Rett syndrome: potential

implications for clinical autonomic dysfunction. J Neuropathol Exp Neurol 64:1018–1027. CrossRef Medline

Pawar A, Nanduri J, Yuan G, Khan SA, Wang N, Kumar GK, Prabhakar NR (2009) Reactive oxygen species-dependent endothelin signaling is required for augmented hypoxic sensory response of the neonatal carotid body by intermittent hypoxia. Am J Physiol Regul Integr Comp Physiol 296:R735–R742. CrossRef Medline

Peña F, Parkis MA, Tryba AK, Ramirez JM (2004) Differential contribution of pacemaker properties to the generation of respiratory rhythms during normoxia and hypoxia. Neuron 43:105–117. CrossRef Medline

Poets CF, Stebbens VA, Alexander JR, Arrowsmith WA, Salfield SA, Southall DP (1991) Oxygen saturation and breathing patterns in infancy. 2: Preterm infants at discharge from special care. Arch Dis Child 66:574–578. CrossRef Medline

Ramirez JM, Quellmalz UJ, Richter DW (1996) Postnatal changes in the mammalian respiratory network as revealed by the transverse brainstem slice of mice. J Physiol 491:799–812. Medline

Ramirez JM, Quellmalz UJ, Wilken B (1997a) Developmental changes in the hypoxic response of the hypoglossus respiratory motor output in vitro. J Neurophysiol 78:383–392. Medline

Ramirez JM, Telgkamp P, Elsen FP, Quellmalz UJ, Richter DW (1997b) Respiratory rhythm generation in mammals: synaptic and membrane properties. Respir Physiol 110:71–85. CrossRef Medline

Ramirez JM, Quellmalz UJ, Wilken B, Richter DW (1998a) The hypoxic response of neurones within the in vitro mammalian respiratory network. J Physiol 507:571–582. CrossRef Medline

Ramirez JM, Schwarzacher SW, Pierrefiche O, Olivera BM, Richter DW (1998b) Selective lesioning of the cat pre-Botzinger complex in vivo eliminates breathing but not gasping. J Physiol 507:895–907. CrossRef Medline

Ramirez JM, Koch H, Garcia AJ 3rd, Doi A, Zanella S (2011) The role of spiking and bursting pacemakers in the neuronal control of breathing. J Biol Phys 37:241–261. CrossRef Medline

Ramirez JM, Garcia AJ 3rd, Anderson TM, Koschnitzky JE, Peng YJ, Kumar GK, Prabhakar NR (2013a) Central and peripheral factors contributing to obstructive sleep apneas. Respir Physiol Neurobiol 189:344–353. CrossRef Medline

Ramirez JM, Ward CS, Neul JL (2013b) Breathing challenges in Rett syndrome: lessons learned from humans and animal models. Respir Physiol Neurobiol 189:280–287. CrossRef Medline

Roux JC, Dura E, Moncla A, Mancini J, Villard L (2007) Treatment with desipramine improves breathing and survival in a mouse model for Rett syndrome. Eur J Neurosci 25:1915–1922. CrossRef Medline

Rukhadze I, Kubin L (2007) Differential pontomedullary catecholaminergic projections to hypoglossal motor nucleus and viscerosensory nucleus of the solitary tract. J Chem Neuroanat 33:23–33. CrossRef Medline

Samaco RC, Mandel-Brehm C, Chao HT, Ward CS, Fyffe-Maricich SL, Ren J, Hyland K, Thaller C, Maricich SM, Humphreys P, Greer JJ, Percy A, Glaze DG, Zoghbi HY, Neul JL (2009) Loss of MeCP2 in aminergic neurons causes cell-autonomous defects in neurotransmitter synthesis and specific behavioral abnormalities. Proc Natl Acad Sci U S A 106:21966–21971. CrossRef Medline

Saper CB, Fuller PM, Pedersen NP, Lu J, Scammell TE (2010) Sleep state switching. Neuron 68:1023–1042. CrossRef Medline

Sarnyai Z, Sibille EL, Pavlides C, Fenster RJ, McEwen BS, Toth M (2000) Impaired hippocampal-dependent learning and functional abnormalities in the hippocampus in mice lacking serotonin(1A) receptors. Proc Natl Acad Sci U S A 97:14731–14736. CrossRef Medline

Schwarzacher SW, Rüb U, Deller T (2011) Neuroanatomical characteristics of the human pre-Botzinger complex and its involvement in neurodegenerative brainstem diseases. Brain 134:24–35. CrossRef Medline

Shao XM, Feldman JL (1997) Respiratory rhythm generation and synaptic inhibition of expiratory neurons in pre-Botzinger complex: differential roles of glycinergic and GABAergic neural transmission. J Neurophysiol 77:1853–1860. Medline

Silvestri JM, Weese-Mayer DE, Hunt CE (2002) Home monitoring during infancy: what is normal? Paediatr Respir Rev 3:10–17. CrossRef Medline

Smith JC, Ellenberger HH, Ballanyi K, Richter DW, Feldman JL (1991) Pre-Bötzinger complex: a brainstem region that may generate respiratory rhythm in mammals. Science 254:726–729. CrossRef Medline

Southall DP, Kerr AM, Tirosh E, Amos P, Lang MH, Stephenson JB (1988) Hyperventilation in the awake state: potentially treatable component of Rett syndrome. Arch Dis Child 63:1039–1048. CrossRef Medline

Spitzer NC (2012) Activity-dependent neurotransmitter respecification. Nat Rev Neurosci 13:94–106. Medline

St-John WM, Leiter JC (2002) Gasping is elicited by briefer hypoxia or ischemia following blockade of glycinergic transmission. Respir Physiol Neurobiol 133:167–171. CrossRef Medline

St-John WM, Paton JF, Leiter JC (2004) Uncoupling of rhythmic hypoglossal from phrenic activity in the rat. Exp Physiol 89:727–737. CrossRef Medline

Takahashi K, Kayama Y, Lin JS, Sakai K (2010) Locus coeruleus neuronal activity during the sleep-waking cycle in mice. Neuroscience 169:1115–1126. CrossRef Medline

Tan W, Janczewski WA, Yang P, Shao XM, Callaway EM, Feldman JL (2008) Silencing preBötzinger complex somatostatin-expressing neurons induces persistent apnea in awake rat. Nat Neurosci 11:538–540. CrossRef Medline

Taneja P, Ogier M, Brooks-Harris G, Schmid DA, Katz DM, Nelson SB (2009) Pathophysiology of locus ceruleus neurons in a mouse model of Rett syndrome. J Neurosci 29:12187–12195. CrossRef Medline

Telgkamp P, Ramirez JM (1999) Differential responses of respiratory nuclei to anoxia in rhythmic brain stem slices of mice. J Neurophysiol 82:2163–2170. Medline

Telgkamp P, Cao YQ, Basbaum AI, Ramirez JM (2002) Long-term deprivation of substance P in PPT-A mutant mice alters the anoxic response of the isolated respiratory network. J Neurophysiol 88:206–213. Medline

Trasande CA, Ramirez JM (2007) Activity deprivation leads to seizures in hippocampal slice cultures: is epilepsy the consequence of homeostatic plasticity? J Clin Neurophysiol 24:154–164. CrossRef Medline

Turrigiano G (2011) Too many cooks? Intrinsic and synaptic homeostatic mechanisms in cortical circuit refinement. Annu Rev Neurosci 34:89–103. CrossRef Medline

Vagedes J, Poets CF, Dietz K (2013) Averaging time, desaturation level, duration and extent. Arch Dis Child Fetal Neonatal Ed 98:F265–F266. CrossRef Medline

Viemari JC, Ramirez JM (2006) Norepinephrine differentially modulates different types of respiratory pacemaker and nonpacemaker neurons. J Neurophysiol 95:2070–2082. Medline

Viemari JC, Roux JC, Tryba AK, Saywell V, Burnet H, Peña F, Zanella S, Bévengut M, Barthelemy-Requin M, Herzing LB, Moncla A, Mancini J, Ramirez JM, Villard L, Hilaire G (2005) Mecp2 deficiency disrupts norepinephrine and respiratory systems in mice. J Neurosci 25:11521–11530. CrossRef Medline

Viemari JC, Garcia AJ 3rd, Doi A, Ramirez JM (2011) Activation of alpha-2 noradrenergic receptors is critical for the generation of fictive eupnea and fictive gasping inspiratory activities in mammals in vitro. Eur J Neurosci 33:2228–2237. CrossRef Medline

Weese-Mayer DE, Lieske SP, Boothby CM, Kenny AS, Bennett HL, Ramirez JM (2008) Autonomic dysregulation in young girls with Rett Syndrome during nighttime in-home recordings. Pediatr Pulmonol 43:1045–1060. CrossRef Medline

Winter SM, Fresemann J, Schnell C, Oku Y, Hirrlinger J, Hülsmann S (2009) Glycinergic interneurons are functionally integrated into the inspiratory network of mouse medullary slices. Pflugers Arch 458:459–469. CrossRef Medline

Winter SM, Fresemann J, Schnell C, Oku Y, Hirrlinger J, Hülsmann S (2010) Glycinergic interneurons in the respiratory network of the rhythmic slice preparation. Adv Exp Med Biol 669:97–100. CrossRef Medline

Zanella S, Roux JC, Viemari JC, Hilaire G (2006) Possible modulation of the mouse respiratory rhythm generator by A1/C1 neurones. Respir Physiol Neurobiol 153:126–138. CrossRef Medline

Zanella S, Mebarek S, Lajard AM, Picard N, Dutschmann M, Hilaire G (2008) Oral treatment with desipramine improves breathing and life span in Rett syndrome mouse model. Respir Physiol Neurobiol 160:116–121. CrossRef Medline

Zhang X, Su J, Rojas A, Jiang C (2010a) Pontine norepinephrine defects in Mecp2-null mice involve deficient expression of dopamine beta-hydroxylase but not a loss of catecholaminergic neurons. Biochem Biophys Res Commun 394:285–290. CrossRef Medline

Zhang ZW, Zak JD, Liu H (2010b) MeCP2 is required for normal development of GABAergic circuits in the thalamus. J Neurophysiol 103:2470–2481. CrossRef Medline

Zoghbi HY, Percy AK, Glaze DG, Butler IJ, Riccardi VM (1985) Reduction of biogenic amine levels in the Rett syndrome. N Engl J Med 313:921–924. CrossRef Medline